Permafrost changes in the northwestern Da Xing'anling Mountains, Northeast China in the past decade

Xiaoli Chang [1, 2★], Huijun Jin[2, 3★], Ruixia He [2*], Yanlin Zhang [1], Xiaoying Li [4], Xiaoying Jin [2] and Guoyu Li [2]

~~[1]School~~[1]School of Earth Science and Spatial Information Engineering, Hunan University of Science and Technology, Xiangtan, Hunan 411201, China,

~~[2]State~~[2]State Key Laboratory of Frozen Soils Engineering, Northwest Institute of Eco-Environment and Resources, Chinese Academy of Sciences, Lanzhou 730000, China,

~~[3]School~~[3]School of Civil Engineering, Institute of Cold-Regions Science and Engineering, and Northeast-China Observatory and Research-Station of Permafrost Geo-Environment (Ministry of Education), Northeast Forestry University, Harbin 150040, China,

~~[4]Key~~[4]Key Laboratory of Sustainable Forest Ecosystem Management (Ministry of Education) and College of Forestry, Northeast Forestry University, Harbin 150040, China

★These authors contributed equally to this work.

Correspondence to: R. He: ruixiahe@lzb.ac.cn

Abstract

Under a pronounced climate warming, permafrost has been degrading in most areas, but it is still unclear in the northwestern part of the Da Xing'anling Mountains, Northeast China. According to a ten-year observation of permafrost and active-layer temperatures, the multi-year average of mean annual ground temperatures at 20 m was −2.83, −0.94, −0.80, −0.70, −0.60 and −0.49 °C, respectively, at Boreholes Gen'he4 (GH4~~, –~~), Mangui3 (MG3~~, –~~), Mangui1 (MG1~~, –~~), Mangui2 (MG2~~, –~~), Gen'he5 (GH5) and Yituli'he2 (YTLH2~~,~~), with the depths of permafrost table varying from 1.1 to 7.0 m. Ground cooling at shallow depths has been detected, resulting in declining thaw depths in Yituli'he during 2009-2020, possibly due to relatively stable mean positive air temperature and declining snow cover and dwindling local population. In most study areas (e.g., Mangui and ~~Genhe~~Gen'he), permafrost warming is particularly pronounced at larger depths (even at 80 m). These results can provide important information for regional development and engineering design and maintenance~~.~~, and also provide a long-term ground temperature dataset for the validation of models relevant to the thermal dynamics of permafrost in Da Xing'anling Mountains. All of the datasets are published through the National Tibetan Plateau Data Center (TPDC), and the link is https://doi.org/10.11888/Geocry.tpdc.271752 (Chang X, 2021).

Key words: Permafrost change, climate warming, ground warming and cooling, declined snow cover, dwindling local population

1 Introduction

带格式的：标题 1，段落间距段前：24 磅，段后：12 磅

带格式的：字体：10 磅，字体颜色：自动设置

Permafrost, defined as ground that remains at or below 0 °C consecutively for two or more years, is widespread in high-latitude and high-elevation regions (Zhang et al., 2007). One quarter of the Northern Hemisphere and 17% of the Earth's currently exposed land surface are underlain by permafrost (Biskaborn et al., 2019). Areal extent of permafrost in China is estimated at about 1.59 $\times 10^6$ km^2 (Youhua et al., 2012), accounting for one sixth of the total Chinese land territories. In northeastern China, land area of about 3.1×10^5 km^2 is underlain by permafrost (Zhang et al., 2021). Northern part of Northeast China is also characterized by the extensive and stable inversion of air temperature in winter, thick surficial deposits, dense vegetation, extensive snow cover, and widespread distribution of wetlands in valley bottoms and lowlands, resulting in strong regional differentiations in permafrost features (Jin et al., 2007). Therefore, the latitudinal permafrost in Northeast China is referred to as the "Xing'an (Hinggan) Baikal permafrost (XBP)" (Jin et al., 2007), a distinct type of ecosystem-dominated permafrost (Shur and Jorgenson, 2007).

Permafrost is sensitive to climate change (Farquharson et al., 2019; Sim et al., 2021; Zhang et al., 2019) and surface disturbances (Guo et al., 2018; Li et al., 2019; Li et al., 2021). Permafrost has experienced significant warming and widespread degradation during the last several decades (Jin et al., 2000; Jin et al., 2007; Shanshan Chen, 2020; Zhang et al., 2019; Jin et al., 2021). It has been evidenced by deeper seasonal thaw (Luo et al., 2018), thinning and warming permafrost (Gruber, 2012; Jin et al., 2021; Jin et al., 2007; Romanovsky et al., 2010), and an areal reduction of permafrost in northeastern China (Li et al., 2021; Zhang et al., 2021). However, most of the regional or local investigations conducted for economic development, engineering design and construction, and environmental management, such as water supply, road construction or coalmining (Jin et al., 2007), would be terminated upon the project completion. Numerous local studies on permafrost changes have been carried out in recent years; howeverPermafrost, defined as ground that remains at or below 0 °C consecutively for two or more years, is widespread in high-latitude and high-elevation regions (Zhang et al., 2007). One quarter of the Northern Hemisphere and 17% of the Earth's currently exposed land surface are underlain by permafrost (Gruber, 2012). Areal extent of permafrost in China is estimated at about 1.59×10^6 km^2 (Youhua et al., 2012), mainly on the Qinghai-Tibet Plateau (about $1.06\text{-}1.17\times 10^6$ km^2) (Zou et al., 2017; Cao et al., 2019), in northeastern China (about 3.1×10^5 km^2) (Zhang et al., 2021) and mountainous areas in northwestern China (Cao et al., 2018). Northern part of Northeast China is also characterized by the extensive and stable inversion of air temperature in winter, thick surficial deposits, dense vegetation, extensive snow cover, and widespread distribution of wetlands in valley bottoms and lowlands, resulting in strong regional differentiations in permafrost features (Jin et al., 2007). Therefore, the latitudinal permafrost in Northeast China is referred to as the “Xing’an (Hinggan)-Baikal permafrost (XBP)” (Jin et al., 2007), a distinct type of ecosystem-dominated permafrost (Shur and Jorgenson, 2007).

Permafrost is sensitive to climate change (Farquharson et al., 2019; Sim et al., 2021; Zhang et al., 2019; Ran et al., 2018) and surface disturbances (Guo et al., 2018; Li et al., 2019; Li et al., 2021). It has experienced significant warming and widespread degradation during the last several decades (Jin et al., 2000; Jin et al., 2007; Zhang et al., 2019; Jin et al., 2021; Chen et al., 2020), evidenced by deeper seasonal thaw (Luo et al., 2018), thinning and warming permafrost (Gruber, 2012; Jin et al., 2021; Jin et al., 2007; Romanovsky et al., 2010), and an areal reduction of permafrost in northeastern China (Li et al., 2021; Zhang et al., 2021). The permafrost change has attracted extensive attention worldwide (Biskaborn et al., 2019), because it has significant potential impacts on the terrestrial eco-hydrological processes (Zhang et al., 2017; Schuur and Mack, 2018; Zhang et al., 2018a; Ala-Aho et al., 2021; Ran et al., 2022) and carbon cycling (Mu et al., 2020; Schuur et al., 2015). In recent decades, huge efforts have been dedicated to developing physically based models to reproduce and predict the thermal dynamic processes of permafrost and their influences. However, lacking long term and systematic in-situ observation of permafrost temperature is an apparent bottleneck for the mentioned relevant analysis and model calibration or validation. The observation in deep ground is especially rare and precious.

As a main distribution region of high latitudes permafrost in China, the intensity and progress on permafrost observation in Da Xing’anling Mountains area was falling far behind other permafrost regions, .e.g., the Qinghai-Tibetan Plateau. Most of such investigation and observation in Da Xing’anling mountains area were aimed at serving some specific short term projects in economic development, engineering design and construction, e.g., road construction and coalmining (Jin et al., 2007), and they were terminated upon the project completion. In recent years, numerous local studies on permafrost change have been carried out. However, most of them have been based on air and/or ground surface temperatures provided by weather stations, reanalysis data ~~(Wei et al., 2011; Zhang et al., 2018; Zhang et al., 2021),~~(Wei et al., 2011; Zhang et al., 2018b; Zhang et al., 2021), or short-term ground thermal observations ~~(He et al., 2021; Jin et al., 2007).~~(He et al., 2021; Jin et al., 2007). Thus, it is hard to more accurately feature and evaluate the latest distribution and future changes of permafrost in Northeast China under the combined influences of warming climate and human activities ~~(Serban et al., 2021).~~

~~Fortunately, similar to the Circumpolar Active Layer Monitoring (CALM) sites(Brown et al.,~~

带格式的: 字体: 10 磅, 字体颜色: 文字 1

带格式的: 字体: 10 磅, 字体颜色: 文字 1

带格式的: 字体: 10 磅, 字体颜色: 文字 1

带格式的: 正文, 左, 行距: 1.5 倍行距

2000; Grebenets et al., 2021; Shiklomanov et al., 2012), or CALM-South sites (Guglielmin, 2006; Guglielmin et al., 2012; Hrbáček et al., 2021), since 2009, a less comprehensive observing system was gradually established at Gen'he, Yituli'he, and Mangui in the northwestern part of the Da Xing'anling Mountains, Northeast China.(Serban et al., 2021). Similar to the Circumpolar Active Layer Monitoring (CALM) sites (Brown et al., 2000; Grebenets et al., 2021; Shiklomanov et al., 2012), or CALM-South sites (Guglielmin, 2006; Guglielmin et al., 2012; Hrbáček et al., 2021), a comprehensive observing system was gradually established since 2009 at Gen'he (GH), Yituli'he (YTLH), and Mangui (MG) in the northwestern part of the Da Xing'anling Mountains, Northeast China. Periodical collection and calibration of data on the thermal regimes of soils in the active layer and permafrost at depths have been carried out in boreholes, generally reaching 20 m in depth and one of them, 80 m, in Gen'he, eastern Inner Mongolia, Northeast China.. This thus presents an opportunity to observe the thermal characteristics of the XAP at depths and to understand and evaluate temporal changes in permafrost features in different landscapes under a warming climate. These results can provide important information for regional planning, development, and engineering design and maintenance in Northeast China. It can also provide a long-term ground temperature dataset for the validation of models relevant to the thermal dynamics of permafrost in Da Xing'anling Mountains.

2 Study area

The Gen'he Station of China Forest Ecological Research Network (CFERN), Yituli'he Permafrost Observatory (YPO), and Mangui Permafrost Station (MPS) are found in the discontinuous permafrost zone of Northeast China (Figure 1), where it is characterized by a cold temperate –continental climate under the influences of alternating monsoons. Multi-year averages of meanannualmean annual air temperature (MAAT) were −–4.0 °C at Gen'he (1961–2020), −–5.2 °C at the YPO (1965–2005) and −–5.8 °C at the MPS (1996–2005). In the same periods, the multi-year average of annual precipitation was 440 mm at Gen'he, 460 mm at the YPO, and 480 mm at the MPS. Annual precipitation falls concentratively in the form of summer rain, according to the chorographic record of Gen'he city. Snowfall (snow water equivalent, or SWE) accounts for about 12~20% of annual total precipitation. Stable snow cover usually starts to occur on the ground surface in the late October and generally

带格式的：字体：10 磅，字体颜色：文字 1
带格式的：字体：10 磅，字体颜色：文字 1
带格式的：字体：10.5 磅，字体颜色：文字 1
带格式的：标题 1，左，段落间距段前：24 磅，段后：12 磅
带格式的：字体：10 磅
带格式的：字体：10 磅，字体颜色：文字 1
带格式的：字体：10 磅，字体颜色：文字 1
带格式的：正文，左，行距：1.5 倍行距
带格式的：字体：10 磅，字体颜色：文字 1
带格式的：字体：10 磅，字体颜色：文字 1
带格式的：字体：10 磅，字体颜色：文字 1
带格式的：字体：10 磅，字体颜色：文字 1
带格式的：字体：10 磅，字体颜色：文字 1
带格式的：字体：10 磅，字体颜色：文字 1
带格式的：字体：10 磅，字体颜色：文字 1
带格式的：字体：10 磅，字体颜色：文字 1
带格式的：字体：10 磅，字体颜色：文字 1
带格式的：字体：10 磅，字体颜色：文字 1
带格式的：字体：10 磅，字体颜色：文字 1

disappears in the next April.

Vegetation differs slightly from site to site where Boreholes GH4, GH5, YTLH1, YTLH2, MG1, MG2 and MG3 are located (Figure 1 and Table 1). Borehole GH4 is in a larch (*Larix gmelinii*) forest, whereas Boreholes GH5, YTLH1, YTLH2 and MG2 are in sedge (*Carex tato*) meadows. The ~~BoreholeMG3~~Borehole MG3 is in an open backyard, and ~~BoreholeMG1~~Borehole MG1, in a birch (*Betula*) shrubland with sedges (*Carex tato*) as an understory. However, soil types are similar (brown coniferous forest soil).–

~~Figure 1. Location of the study area and the distribution of borehole sites in the zones of frozen ground in the northern Da Xing'anling Mountains, Northeast China~~

Among the seven boreholes, Borehole YTLH1 of 8.15 m in depth was first installed for monitoring the hydrothermal dynamics of active layer and shallow permafrost at the end of 2008, with weekly manual measurement of soil temperatures since 2009. However, in order to monitor the permafrost temperature at the depth of zero annual amplitude (generally at 10-25 m in Northeast China), an additional borehole (YTLH2) was drilled to a depth of 20 m at a nearby site (10 m away from the YTLH1) with almost identical physical and vegetative conditions on the ground surface. The thermistor cables were permanently installed for manually monitoring ground temperatures since 2010. Boreholes GH4, GH5, MG1, MG2 and MG3 have been monitored since the beginning of 2012, but for different observational frequencies (Table 1). These thermistor cables were assembled by the State Key Laboratory of Frozen Soils Engineering (SKLFSE), Cold and Arid Regions Environmental and Engineering Research Institute (CAREERI; now renamed to the Northwest Institute of Eco-Environment and Resources, or NIEER), Chinese Academy of Sciences (CAS), Lanzhou, China, with an accuracy of ±0.05 °C in the temperature range from –30 to +30 °C, and ±0.1 °C, from –45 to –30 °C and +30 to +50°C.

For continuous observation, data for ground temperatures at the Borehole GH4 were automatically collected hourly by the Micrologger CR3000 (USA), whereas at other sites were manually measured with a multi-meter (Fluke 189®). Unfortunately, not all records for soil temperature are complete for all boreholes. For example, there were two hiatuses for the records of Borehole GH4 (2014-2016 and 2017-2019) due to the logger damage. Manual records from January to June in 2014 for other boreholes were lost in mailing. The measurement at MG3 was halted in 2016 because of borehole damage and that at GH5 and YTLH2, in 2020, due to the outbreak of the COVID-19 virus and the ensued traffic control.

带格式的: 字体: 10 磅, 字体颜色: 文字 1
带格式的: 字体: TimesNewRomanPS-ItalicMT, 10 磅, 字体颜色: 文字 1
带格式的: 字体: 10 磅, 字体颜色: 文字 1
带格式的: 字体: 10 磅, 字体颜色: 文字 1
带格式的: 字体: 10 磅, 字体颜色: 文字 1
带格式的: 字体: TimesNewRomanPS-ItalicMT, 10 磅, 字体颜色: 文字 1
带格式的: 字体: 10 磅, 字体颜色: 文字 1
带格式的: 字体: 10 磅, 字体颜色: 文字 1
带格式的: 字体: 10.5 磅, 字体颜色: 文字 1
带格式的: 正文, 居中
带格式的: 字体: 10 磅, 字体颜色: 文字 1
带格式的: 正文, 左, 行距: 1.5 倍行距
带格式的: 字体: 10 磅, 字体颜色: 文字 1
带格式的: 字体: 10 磅, 字体颜色: 文字 1
带格式的: 字体: 10 磅, 字体颜色: 文字 1
带格式的: 字体: 宋体, 10 磅, 字体颜色: 文字 1
带格式的: 字体: 10 磅, 字体颜色: 文字 1
带格式的: 字体: 10 磅, 字体颜色: 文字 1
带格式的: 字体: 10 磅, 字体颜色: 文字 1

The specifics are presented in Table 1.

~~Table 1. Characteristics and monitoring information of ground temperature boreholes in the northwestern part of Da Xing'anling Mountains, Northeastern China~~

3 Results

3.1 Ground temperatures in near-surface permafrost and active layer

Ground temperatures of near-surface soil (e.g., at depths of 1 and 2 m) responds quickly to changes in air temperature, but the change patterns of ground temperatures show a reduction of amplitude with increasing depth in all these boreholes. In Boreholes GH4, MG3, YTLH1 and YTLH2, seasonal variations in ground temperature still could be detected at the depth of 5 m. However, at depths of 3 and 4 m, variations in winter ground temperatures gradually flattens out in Boreholes GH5, MG1 and MG2, and only the annual variability in summer ground temperatures can be detected at the depth of 5 m (Figure 2). Therefore, only a small temperature amplitude (0.5~1.0°C) was detected at the depth of 5 m in comparison with that at 3 m (2~3°C).

~~Figure 2. Variability of measured ground temperatures at depths of 1-5 m for Boreholes GH4 and GH5 (a)), MG1, MG2 and MG3 (b)), and YTLH1 and YTLH2 (c)).~~

Based on the thermal observation at ~~BoreholeMG1~~Borehole MG1, 2.6 m (2017) and 1.9 m (2020) in depth were respectively the maximum and minimum depths of the permafrost table~~.~~ (Table 2). Combining the data in Figure 2b and other observational data, the active layer thickness (ALT) at Borehole MG2 increased from 4.3 m (2012) to 4.8 m (2016), but thinned to 4.2 m (2019) afterwards. The permafrost table at MG3 was located at 2.8 m (2012 and 2013), 4.0 m (2014) and 3.3 m (2015) in depth during the observation period. Subtle freeze-thaw cycles were observed at 2.0 m in depth in Borehole GH4 (Figure 2a), and the 0 °C isotherms in Figure 3a indicated a range of ALT from 2.2 m (2016) to 2.0 m (2018). In Borehole GH5, despite of a small temperature range (0.5°C) at the depth of 6.0 m, freeze-thaw cycles took place. During the monitoring period, the sensor at 7.0 m in depth showed all negative temperatures, but in the left proximity of 0 °C, all year round, with a multi-year average of mean annual soil temperature at −0.08°C. The thawing front reached down to the depth of 7.0 m every

带格式的：字体：10 磅
带格式的：字体：10 磅
带格式的：标题 1，左，段落间距段前：24 磅，段后：12 磅
带格式的：字体：Times New Roman，10 磅
带格式的：标题 2，左，段落间距段前：12 磅，段后：12 磅
带格式的：字体：Times New Roman，10 磅
带格式的：字体：10 磅，字体颜色：文字 1
带格式的：正文，左，行距：1.5 倍行距
带格式的：字体：10 磅，字体颜色：文字 1
带格式的：字体：10 磅，字体颜色：文字 1
带格式的：字体：10 磅，字体颜色：文字 1
带格式的：字体：10 磅，字体颜色：文字 1
带格式的：字体：10 磅，字体颜色：文字 1
带格式的：字体：10 磅，字体颜色：文字 1
带格式的：字体：10 磅，字体颜色：文字 1
带格式的：正文，左，行距：1.5 倍行距
带格式的：字体：10 磅，字体颜色：文字 1
带格式的：字体：10 磅，字体颜色：文字 1
带格式的：字体：10 磅，字体颜色：文字 1
带格式的：字体：10 磅，字体颜色：文字 1，下标
带格式的：字体：10 磅，字体颜色：文字 1
带格式的：字体：10 磅，字体颜色：文字 1
带格式的：字体：10 磅，字体颜色：文字 1
带格式的：字体：10 磅，字体颜色：文字 1
带格式的：字体：10 磅，字体颜色：文字 1
带格式的：字体：10 磅，字体颜色：文字 1
带格式的：字体：10 磅，字体颜色：文字 1
带格式的：字体：10 磅，字体颜色：文字 1
带格式的：字体：10 磅，字体颜色：文字 1
带格式的：字体：10 磅，字体颜色：文字 1

year (Figure 3b), which means the permafrost table here has been lowered to 7.0 m in depth. In Borehole YTLH1, ground thaw occurred occasionally at 2.0 m, for an example, in October 2016, but the ALT mostly varied from 1.5 m (2011) to 1.0 m (2017) during the observation (Figure 3c). In the same period in 2016, −-0.1 °C was registered as the highest temperature at 2.0 m in depth in Borehole YTLH2 (Figure 2c), but an above-zero temperature, at 1.5 m depth. The depth of the permafrost table fluctuated between 1.6 m (2017) and 2.0 m (2011 and 2016) (Figure 3d and Table 2).

Figure 3 Variability of 0 °C isotherms (black curves) of ground temperature for Boreholes GH4 (a), GH5 (b), YTLH1 (c), and YTLH2 (d). The empty space indicates the period of missing data.

3.2 Change trends of permafrost temperature at depths

Figure 4 highlights the changes in thermal regimes of permafrost at different depths in Boreholes MG1, MG2 and MG3. Ground temperature was on the rise, but its amplitude decreased with depth since the beginning of observation in 2012. The depth of zero annual amplitude (ZAA) was estimated to be the place where ground temperature changes by no more than 0.1°C throughout a year (Everdingen, 1998 (revised 2005)). Although the ground temperature was not measured periodically with a very fine time step and some values were lost, the estimation could still be reasonable, because the temperature fluctuation in deep ground is significantly dampened. According to the monitoring data, the depth of ZAA varies among different boreholes (Table 2) without considering interannual changes. In order to show more accurate thermal statses of permafrost, ground termperatures of 20m were chosen to compare within different boreholes in this paper. In Borehole MG1, the amplitude of ground temperatures below 8 m in depth was no more than 0.4 °C, and seasonal variability was hardly detectable at depths of 16 and 20 m. The results of linear fitting (red trend lines) indicate an overall warming trend of permafrost during 2012-2020. A mulit-year average of mean annual ground temperature (MAGT, at 20 m; from 2012 to 2020) of −-0.877 °C was obtained in Borehole MG1. In Borehole MG2, ground temperature varied slightly (±(±0.06°°C) with the seasons even at the depth of 20 m, where the MAGT was about −-0.769 °C. Permafrost here was also warming, with a rising amplitude of 0.1~0.2 °C from 2012 to 2020. The valid monitoring period was less than 5 years in Borehole MG3 (1 January 2012 to 29 April 2016), when the largest ground temperature range of 0.2-0.5 °C was detected between 8 m and 20 m. Similar to the Borehole MG2, pemafrost at 20 m in depth in Borehole MG3 has been experiencing some seasonal variations, with a multi-year average of MAGT at ~~−~~−0.~~9~~94 °C~~.~~ (Table 2).

~~Figure 4. Variability of permafrost temperatures at depths of 8, 10, 12, 16 and 20 m in Boreholes MG1, MG2 and MG3 in Mangui, northern Da Xing'anling Mountains, Northeast China during 2012-2020. GT stands for ground temperature.~~

Permafrost at depths of 8 and 20 m in Boreholes GH4 and GH5 (Figure 5) warmed by 1.5~~-~~-0.2 and 0.2~~–~~-0.1°C, respectively, during 2012-2020. The warming of permafrost at GH5 was insignificant in comparison with that at other sites. Mean annual soil temperature at 8 m in depth have slightly warmed from ~~−~~−0.17 °C in 2012 to ~~−~~−0.16 °C in 2019, and; the MAGT at 20 m in depth, from ~~−~~−0.60 to ~~−~~−0.57 °C over the same period. MAGT at 20 m in depth was averaged at ~~−~~−0.59 °C during 2012-2019. However, permafrost at GH4 was relatively cold, with a multi-year average of MAGT at ~~−~~−2.~~83~~84 °C at 20 m in depth. According to Figure 5, ground temperatures fluctuated seasonally at above 20 m in depth. However, seasonal variations in ground temperature dwindled gradually below 30 m (Figure 6), leaving only inter-annual variations. Ground temperatures in Borehole GH4 increased with increasing depth (~~−~~(−2.51, ~~−~~−1.76 and ~~−~~−0.41 °C at 30, 50 and 80 m, respectively), whereas the thermal fluctuations declined downwards (0.2 °C at 20 and 30 m in depth, but 0.03 °C at 80 m). Thus, during 2012-2020, the ground at depths of 30-80 m at the GH4 site was warming at an average rate of 0.~~004~~04-0.~~020~~20 °C /~~yr.~~ dec.

~~Figure 5. Variations in permafrost temperatures at depths of 8, 10, 12, 16 and 20 m in Boreholes GH4 and GH5 in Gen'he, northern Da Xing'anling Mountains, Northeast China during 2012-2020. GT stands for ground temperature.~~

~~Figure 6. Variability of deep permafrost temperatures at depths of 30 – 80 m for Borehole GH4 in Gen'he, northern Da Xing'anling Mountains, Northeast China during 2012-2020. GT stands for ground temperature.~~

In Borehole YTLH2, remarkable seasonal variations were noted at each measured depth. The seasonal amplitude of ground temperature gradually dampened with increasing depth, varying from approximately 0.5 °C at 8 m in depth to less than 0.1 °C at 20 m. Unlike permafrost in Mangui town and Gen'he city, a significant cooling of permafrost was detected at all depths except 20 m at YTLH2 during the 10-year observation (Figure 7). The average rate of temperature change at 20 m depth is close to 0 °C /~~yr~~dec and the MAGT here has been roughly maintained at ~~−~~−0.49 °C in the past decade~~.~~ (Table 2).

带格式的 ...

带格式的：字体：10 磅，字体颜色：文字 1

带格式的 ...

带格式的：正文，左，行距：1.5 倍行距

带格式的：字体：10 磅，字体颜色：文字 1

带格式的：正文，左，行距：1.5 倍行距

带格式的 ...

~~Figure 7. Variability of permafrost temperatures at depths of 8, 12, 16 and 20 m at Borehole YTLH2 in Yituli'he in northern Da Xing'anling Mountains, Northeast China during 2012-2020. GT stands for ground temperature.~~

4 Discussion

4.1 Change trends of near-surface permafrost temperatures

Based on the analysis in Section 3.1, it can be inferred that changes in the ground thermal regimes of the ecosystem-dominated permafrost on the northwestern slope of the Da Xing'anling Mountains are mainly controlled by changes in local factors, such as vegetation and snow covers and human activities, especially in the ~~active layer thickness (ALT).~~ALT. For example, ALT ranges from 2.5 m in 2016 and 2017 to 1.9 m in 2020 for the site in shrubs (MG1), 4.8 m in 2017 to 4.2 m in 2020 in sedge meadow (MG2) and 2.9 m in 2012 to 4.0 m in 2014 in the farmer's backyard (MG3) during the observation period. Apparently, the Borehole MG1, far away from downtown Mangui, had the least ALT because of more shading effect of shrubs than that of meadow (MG2) and less anthropogenic impact than that of backyard (MG3). Declining trend of ALT was also observed in the Nanwenghe Wetlands Reserve on the southern slope of the Da Xing'aning-Yile'huli Mountain Knots, Northeast China, probably driven by a rising surface and thermal offsets of vegetation cover and organic soils ~~(He et al., 2021).~~(He et al., 2021). Additionally, at the MG3 site, the smaller ALT could be attributed to the shading effect of the farmer's house and more heat loss to the atmosphere caused by snow removal in the yard in winter as well. In Gen'he, at the site of Borehole GH4 in a primeval forest, ALT remained unchanged at 2.2 m from 2012 to 2016 and, without human disturbance, permafrost was well-preserved. On the contrary, at the GH5 site in the suburb meadow frequently disturbed by the nearby livestock, a complex thermal regime was observed in the active layer. Ground temperatures at the depths of 3.5-6.0 m were negative from March to September and positive in other time every year, and; not until 7.0 m in depth, where it became below $0^{o}C$ all the year round. By definition, the active layer is the layer above permafrost that freezes in winter and thaws in summer. Therefore, 7 m is supposed to be the reasonable ALT or the depth of the permafrost table, and there might be no supra-permafrost subaerial talik ~~(Jin et al., 2021)~~(Jin et al., 2021) between the active layer and the permafrost table at this site, i.e., attached permafrost. However, the supra-

带格式的：字体：10 磅
带格式的：标题 1，左，段落间距段前：24 磅，段后：12 磅
带格式的：字体：10 磅
带格式的：标题 2，左，段落间距段前：12 磅，段后：12 磅
带格式的：字体：Times New Roman，10 磅，非倾斜
带格式的：字体：Times New Roman，10 磅
带格式的：字体：10 磅，字体颜色：文字 1
带格式的：正文，左，行距：1.5 倍行距
带格式的：字体：10 磅，字体颜色：文字 1
带格式的：字体：10 磅，字体颜色：文字 1
带格式的：字体：宋体，10 磅，字体颜色：文字 1
带格式的：字体：10 磅，字体颜色：文字 1
带格式的：字体：10 磅，字体颜色：文字 1

permafrost subaerial talik, which has appeared in the Nanwenghe Wetlands Reserve about 300 km to the east of the study site ~~(He et al., 2021),~~(He et al., 2021), may develop at this site in the future. In Yituli'he, the two boreholes (YTLH1 and YTLH2) are, about 20 m apart, both in the meadowy swamp to the east of the railway and to the west of highway. Permafrost here is well developed, partially thanks to the sufficient moisture provided by lowland swamp, which also possibly facilitates the formation of ice wedges ~~(Yang and Jin, 2011).~~ (Yang and Jin, 2011).

Notably, there was a decreasing trend in ground temperatures at shallow depths no matter in summer or winter during 2010-2020 (Figure 2), otherwise suggesting a cooling permafrost at ~~-~~shallow depths in the last decade on the northwestern slope of the Da Xing'anling Mountains if no ground-surface conditions are taken into account. The maximum thaw depth (MTD) in Yituli'he rose gradually with fluctuations during 1980-2005, and it showed a downward trend during 2010-2019 (Figure 8). This could be related to the thriving vegetation, and declining winter precipitation ~~and~~or snow cover in this area during the observational period. ~~Figure 8b shows a barely changed~~ In the last decade, although the mean positive air temperature (MPAT) barely changed in Gen'he ~~in the past decade, but~~(Fig 9b), precipitation in warm seasons increased slightly, leading to a wetter condition in favor of vegetation thriving. For example, the maximum vegetation height of *Carex tato* at YTLH1 and YTLH2 grew significantly from 2009 to 2014. Bushes have also emerged recently near the borehole. Thriving vegetation will reduce the solar irradiance incident onto the soil surface in summer and cast a cooling effect on the ground temperature. On the contrary, the winter precipitation (Figure ~~8a~~9a) and snow cover, including the maximal snow depth (Figure ~~8c~~9c) and snow duration (Figure ~~8d~~9d), declined slightly~~,~~ ~~driving the cooling of shallow~~. The thermal insulation effect of snow cover will be weakened when the snow the depth of snow cover decreased, which will lead to a larger heat removal from the permafrost ~~in this region. In addition, the maximum thaw depth (MTD) in Yituli'he was rising but with fluctuations during 1980-2005, but it presented a fluctuating downward trend during 2009-2020 (Figure 9), also implying a cooling of shallow~~to air in winter and drive the permafrost cooling. The detail mechanisms for the cooling permafrost will be further investigated with the help of some physically based models after complementing observations on the interactions of energy balance between the permafrost, vegetation, and snow cover.

~~Figure 8. Climatic characteristics of Gen'he on the northwestern flank of the northern Da~~

~~Xing'anling Mountains in Northeast China in the past ten years~~

~~Figure 9. The maximum thaw depth in Yituli'he on the northwestern flank of the northern Da Xing'anling Mountains in Northeast China between 1980-2020 (Black squares appeared in the paper from Jin et al. (2007), red ones are obtained in this observation. The two boreholes are 10 m from each other, with similar surface, hydrology and soil conditions.)~~

4.2 Change trends of permafrost temperatures at larger depths

Permafrost in Mangui

During the observation period, the averages of MAGTs at the depth of 20 m were −0.79, −0.70 and −0.93 °C, respectively, in shrubs (MG1), meadow (MG2) and farmer's backyard, indicating a poor correlation between the thermal state of deeper permafrost and vegetation cover or anthropic disturbances. However, there was a close relationship between permafrost change at larger depths and land surface conditions. Permafrost below 8 m was significantly warming in the last decade under a warming climate (Figure 4). In Borehole-MG1 and Borehole-MG2 in particular, the rates of ground warming increased slightly with depth (<0.~~03 °C/a~~3 °C/dec for MG1 and <0.~~02 °C/a~~2 °C/dec for MG2), demonstrating a less significant thermal rising in deeper permafrost. Within the zone of discontinuous permafrost, the negative relationship between effective leaf area index (LAI_e) and soil moisture may contribute to differential rates of permafrost thaw ~~(Baltzer et al., 2014).~~(Baltzer et al., 2014). Therefore, more effective water uptake by shrubs than meadow results in lower soil moisture, leading to a more rapid thaw of permafrost at the MG1 site than that at the MG2 site. The warming rate of permafrost in Borehole MG3, with a large warming range, decreased with depth (0.~~05 °C/a~~5 °C/dec at depths of 10 and 12 m, but approximately 0.~~02 °C/a~~2 °C/dec at depths of 16 and 20 m), probably due to short monitoring period and less data. However, it does verify that, in Mangui, permafrost at depths is warming or degrading in the last decade.

Permafrost in Gen'he

Indeed, there exists some long periods with missing data at GH4, and it is reluctant to make the trend analysis with these missing data. However, at the surface layers, although the fluctuation of ground temperature is relatively huge, the collected data has generally captured the maximal and minimal ground temperature in years with observing data. Simply by a visual inspection, the minimal or maximal ground

带格式的: 字体: Times New Roman, 10 磅, 非倾斜
带格式的: 字体: Times New Roman, 10 磅
带格式的: 标题 2, 左, 段落间距段前: 12 磅, 段后: 12 磅
带格式的: 字体: 10 磅, 字体颜色: 文字 1
带格式的: 正文, 左, 段落间距段前: 0.5 行, 段后: 0.5 行
带格式的: 字体: 10 磅, 加粗, 字体颜色: 文字 1
带格式的: 字体: 10 磅, 字体颜色: 文字 1
带格式的: 正文, 左, 行距: 1.5 倍行距
带格式的: 字体: 10 磅, 字体颜色: 文字 1
带格式的: 字体: 10 磅, 字体颜色: 文字 1
带格式的: 字体: 10 磅, 字体颜色: 文字 1
带格式的: 字体: 宋体, 10 磅, 字体颜色: 文字 1
带格式的: 字体: 10 磅, 字体颜色: 文字 1
带格式的: 字体: 10 磅, 字体颜色: 文字 1
带格式的: 字体: 10 磅, 字体颜色: 文字 1
带格式的: 字体: 10 磅, 字体颜色: 文字 1, 下标
带格式的: 字体: 10 磅, 字体颜色: 文字 1
带格式的: 字体: 10 磅, 字体颜色: 文字 1
带格式的: 字体: 10 磅, 字体颜色: 文字 1
带格式的: 字体: 10 磅, 字体颜色: 文字 1
带格式的: 字体: 10 磅, 字体颜色: 文字 1
带格式的: 字体: 10 磅, 字体颜色: 文字 1
带格式的: 正文, 左, 段落间距段前: 0.5 行, 段后: 0.5 行
带格式的: 字体: 10 磅, 加粗, 字体颜色: 文字 1

temperature has an apparent warming trend from 2012 to 2020, which has a good coincidence with the trend analysis in this study. That is, although the missing values could make some loss for the accuracy of trending analysis, or make it less robust, they will not change the trend in an antipodal way. In addition, in depths greater than 8 m, the annual fluctuation of ground temperature was much less than the surface layers, as shown in Figure 5 and 6. The missing values will not vary too much from the collected values. Therefore, we speculate the influence of missing values on trending analysis for deep layers will be smaller than that in the surface layers, and it will decrease with depth, which can be inferred from Figure 5 and 6.

In Borehole GH4, lower ground temperatures and greater warming range was observed in comparison with those in Borehole GH5 in the last decade (Figure 45). Even at depths of 70 and 80 m, ground temperatures were still rising with time at appreciable warming rates (Figure 56), reflecting the impact of climatic warming on permafrost at greater depths. A subtle warming trend of permafrost at depths of 8-20 m in Borehole GH5 was also detected with a rate of 0.004 °C/a04 °C/dec during the observation period (Figure 45). This warming rate of ground temperature is similar to that of the Borehole 85-8A in the southern zone of discontinuous permafrost in North America, where the permafrost is often vertically in isothermal condition and close to 0 °C in ground temperature (Smith et al., 2010).(Smith et al., 2010). In this situation, latent heat effects are considered as the key factor for leading to isothermal conditions in the ground and allowing permafrost to persist under a warming climate (Smith et al., 2010).(Smith et al., 2010). If the effect of large thermal inertia lasts long enough, the supra-permafrost subaerial talik will be highly likely to form and permafrost will be gradually buried. In a word, permafrost degradation in Gen'he is also evident at present in both forested landscape and anthropic zones, particularly in the latter one.

Permafrost in Yituli'he

According to previous study (Jin et al., 2007).(Jin et al., 2007), MAGT at 13 m in Yituli'he rose by 0.2 °C during 1984-1997, continuously rising from −-1.00 °C in 1997 to −-0.55 °C in 2010, except during the short suspension of monitoring (2005-2008), and peaking at −-0.53 °C in 2013. After that, it kept lowering consecutively and by 2018 it was lower than −-0.70 °C, showing an evident cooling trend of permafrost in a sharp contrast to the ground warming trends in Gen'he, Mangui, and other permafrost regions in the world (Douglas et al., 2021; Farquharson et al., 2019).(Douglas et al., 2021;

带格式的：字体：10 磅，字体颜色：文字 1
带格式的：正文，左，行距：1.5 倍行距
带格式的：字体：10 磅，字体颜色：文字 1
带格式的：字体：10 磅，字体颜色：文字 1
带格式的：字体：10 磅，字体颜色：文字 1
带格式的：字体：10 磅，字体颜色：文字 1
带格式的：字体：10 磅，字体颜色：文字 1
带格式的：字体：10 磅，字体颜色：文字 1
带格式的：字体：10 磅，字体颜色：文字 1
带格式的：正文，左，段落间距段前：0.5 行，段后：0.5 行
带格式的：字体：10 磅，加粗，字体颜色：文字 1
带格式的：字体：10 磅，字体颜色：文字 1
带格式的：正文，左，行距：1.5 倍行距
带格式的：字体：10 磅，字体颜色：文字 1
带格式的：字体：10 磅，字体颜色：文字 1
带格式的：字体：10 磅，字体颜色：文字 1
带格式的：字体：10 磅，字体颜色：文字 1
带格式的：字体：10 磅，字体颜色：文字 1

Farquharson et al., 2019). Based on the investigation, there was once a Railway Branch Administration in Yituli'he town since 1964s to 1970s, with a population of over 30,000, but the branch was terminated in 1998. After that, more and more people emigrated and less than 10,000 residents have remained at present, thus leaving a chance for restoration of the local eco-environment and for recovering permafrost temperature.

So far, the mitigation of permafrost degradation becomes considerably difficult in the context of a persistent climate warming ~~(Brown et al., 2015; Luo et al., 2018).~~(Brown et al., 2015; Luo et al., 2018). However, within the dried margin of the Twelvemile Lake (66°27′N, 145°34′W), permafrost aggradation has taken place due to willow shrub uptake of summer recharge and summer shading recharge reduction ~~(Briggs et al., 2014). Beer et al. (Beer et al., 2020)~~(Briggs et al., 2014). Beer et al. (Beer et al., 2020) also found that most permafrost-affected soil could be preserved by increasing the population density of big herbivores in northern high-latitude ecosystems as a result of reducing insulation of winter snow cover. The fact that permafrost is cooling in Yituli'he demonstrates that the ecosystem-protected permafrost in discontinuous permafrost zone may recover if the disturbances, such as human activities, dwindle. Thus, our research results would provide key evidence for the preservation of permafrost in areas with intense past anthropic disturbances ~~(Serban et al., 2021).~~ (Serban et al., 2021).

5 Conclusions

Long-term records of permafrost monitoring presented here from the northwestern flank of the Da Xing'anling Mountains in Northeast China show some important characteristics of ground thermal regimes in the past eight years (2012-2020). The lowest MAGT at 20 m in depth was ~~=~~−2.83 °C in Borehole GH4 in a primeval larch forest, and ~~=~~−0.94, ~~=~~−0.80, ~~=~~−0.70, ~~=~~−0.60 and ~~=~~−0.49 °C, respectively, at MG3, MG1, MG2, GH5 and YTLH2. The maximum of the burial depth of the permafrost table at about 7.0 m was discovered in Borehole GH5, and the minimum, 1.1 ~ 1.5 m at YTLH1. The permafrost table was at depths of about 2.0 m at GH4 and YTLH2, and 2.5, 5.0 and 4.0 m at MG1, MG2 and MG3, respectively. Local factors, such as vegetation and snow covers and human activities, are supposed to be mainly responsible for the changes in the ALT and the thermal state of shallow permafrost

带格式的：字体：10 磅，字体颜色：文字 1
带格式的：字体：10 磅，字体颜色：文字 1
带格式的：字体：10 磅，字体颜色：文字 1
带格式的：字体：10 磅，字体颜色：文字 1
带格式的：字体：10 磅，字体颜色：文字 1
带格式的：字体：10 磅，字体颜色：文字 1
带格式的：字体：10 磅
带格式的：标题 1，左，段落间距段前：24 磅，段后：12 磅
带格式的：字体：10 磅
带格式的：字体：10 磅，字体颜色：文字 1
带格式的：正文，左，行距：1.5 倍行距
带格式的：字体：10 磅，字体颜色：文字 1
带格式的：字体：10 磅，字体颜色：文字 1
带格式的：字体：10 磅，字体颜色：文字 1
带格式的：字体：10 磅，字体颜色：文字 1
带格式的：字体：10 磅，字体颜色：文字 1
带格式的：字体：10 磅，字体颜色：文字 1

in the study area. The most important fact is that ground cooling at shallow depths, as well as the declining ALT in Yituli'he after 2009, has been detected during the observation period, which is probably caused by fairly constant MPAT (mean positive air temperature) and weakened insulation of winter snow cover.

Apart from Yituli'he, permafrost warming at large depths was particularly pronounced during the observation period, even at depths of 70 and 80 m, with different ground warming rates. It is noteworthy that geothermal gradient at depths in Borehole GH5 is almost zero (vertically no change) and with MAGT at about 0 ℃ due to huge thermal inertia of the ice-rich permafrost. This may most likely lead to the formation of the supra-permafrost subaerial talik soon. At the Yituli'he Permafrost Observatory, permafrost has been cooling since the re-establishment of monitoring ~~programin~~program in 2010; the rapidly declining local population might have relieved its stress on the eco-environment and resulted in permafrost recovery. This fact makes it possible to mitigate the permafrost degradation in the zone of ecosystem-dominated permafrost, offering a new thought for permafrost protection.

Author Contributions

XC, HJ, and RH designed the study. XC wrote the manuscript and performed the analysis. YZ plotted the figures. XL, XJ and GL contributed parts of the field data. HJ improved the writing and structure of the paper.

Competing interests

The contact author has declared that neither they nor their co-authors have any competing interests.

Disclaimer

Special issue statement

This article is part of the special issue "Extreme environment datasets for the three poles". It is not associated with a conference.

带格式的：字体：10 磅，字体颜色：文字 1
带格式的：字体：10 磅，字体颜色：文字 1
带格式的：字体：10 磅
带格式的：字体：10 磅，非加粗，字体颜色：文字 1
带格式的：标题 1，左，段落间距段前：24 磅，段后：12 磅
带格式的：字体颜色：文字 1
带格式的：正文，左，段落间距段前：0.5 行，段后：0.5 行
带格式的：字体：10 磅
带格式的：标题 1，左，段落间距段前：24 磅，段后：12 磅
带格式的：字体：10 磅，字体颜色：文字 1
带格式的：字体：7.5 磅，字体颜色：文字 1
带格式的：字体颜色：文字 1
带格式的：正文，左，段落间距段前：0.5 行，段后：0.5 行
带格式的：字体颜色：文字 1
带格式的：字体：10 磅
带格式的：标题 1，左，段落间距段前：24 磅，段后：12 磅
带格式的：字体：10 磅，非加粗，字体颜色：文字 1
带格式的：字体颜色：文字 1
带格式的：正文，左，段落间距段前：0.5 行，段后：0.5 行
带格式的：字体颜色：文字 1
带格式的：字体：10 磅，字体颜色：文字 1
带格式的：标题 1，左，段落间距段前：24 磅，段后：12 磅
带格式的：字体：10 磅
带格式的：字体：10 磅，字体颜色：文字 1
带格式的：字体：7.5 磅，字体颜色：文字 1
带格式的：字体颜色：文字 1
带格式的：正文，左，段落间距段前：0.5 行，段后：0.5 行
带格式的：字体：Times New Roman，字体颜色：文字 1
带格式的：字体颜色：文字 1
带格式的：字体颜色：文字 1
带格式的：字体颜色：文字 1

Acknowledgements

Thanks go to the Inner Mongolia Agricultural University for fieldwork support and the Gen'he Weather Bureau for meteorological data provision. This study was financially supported by the National Natural Science Foundation of China (Grant Nos. 41971079, 41671059, 41871052 and U20A2082) and the Natural Science Program of Hunan Province (Grant No. 2020JJ5161).

Data availability

Chang, X.: Geotemperature observation data set of Genhe River (2012-2019), The dataset is available from the National Tibetan –Plateau/Third Pole Environment Data Center [data set], DOI: (https://doi.org/10.11888/Geocry.tpdc.271752, Chang X, 2021.).

Reference

Baltzer, J. L., Veness, T., Chasmer, L. E., Sniderhan, A. E., and Quinton, W. L.: Forests on thawing permafrost: fragmentation, edge effects, and net forest loss, Global change biology, 20, 824-834, 10.1111/gcb.12349, 2014.

Beer, C., Zimov, N., Olofsson, J., Porada, P., and Zimov, S.: Protection of Permafrost Soils from Thawing by Increasing Herbivore Density, Scientific reports, 10, 4170, 10.1038/s41598-020-60938-y, 2020.

Biskaborn, B. K., Smith, S. L., Noetzli, J., Matthes, H., Vieira, G., Streletskiy, D. A., Schoeneich, P., Romanovsky, V. E., Lewkowicz, A. G., Abramov, A., Allard, M., Boike, J., Cable, W. L., Christiansen, H. H., Delaloye, R., Diekmann, B., Drozdov, D., Etzelmüller, B., Grosse, G., Guglielmin, M., Ingeman-Nielsen, T., Isaksen, K., Ishikawa, M., Johansson, M., Johannsson, H., Joo, A., Kaverin, D., Kholodov, A., Konstantinov, P., Kröger, T., Lambiel, C., Lanckman, J.-P., Luo, D., Malkova, G., Meiklejohn, I., Moskalenko, N., Oliva, M., Phillips, M., Ramos, M., Sannel, A. B. K., Sergeev, O., Seybold, C., Skryabin, P., Vasiliev, A., Wu, Q., Yoshikawa, K., Zheleznyak, M., and Lantuit, H.: Permafrost is warming at a global scale, Nature Communications, 10, 264, 10.1038/s41467-018-08240-4, 2019.

Briggs, M. A., Walvoord, M. A., McKenzie, J. M., Voss, C. I., Day-Lewis, F. D., and Lane, J. W.: New permafrost is forming around shrinking Arctic lakes, but will it last?, Geophysical Research Letters, 41, 1585-1592, https://doi.org/10.1002/2014GL059251, 2014.

Brown, D. R. N., Jorgenson, M. T., Douglas, T. A., Romanovsky, V. E., Kielland, K., Hiemstra, C., Euskirchen, E. S., and Ruess, R. W.: Interactive effects of wildfire and climate on permafrost degradation in Alaskan lowland forests, Journal of Geophysical Research: Biogeosciences, 120, 1619-1637, https://doi.org/10.1002/2015JG003033, 2015.

Brown, J., Hinkel, K. M., and Nelson, F. E.: The circumpolar active layer monitoring (calm) program: Research designs and initial results, Polar Geography, 24, 166-258, 10.1080/10889370009377698, 2000.

Douglas, T. A., Hiemstra, C. A., Anderson, J. E., Barbato, R. A., Bjella, K. L., Deeb, E. J., Gelvin, A. B., Nelsen, P. E., Newman, S. D., Saari, S. P., and Wagner, A. M.: Recent degradation of interior Alaska permafrost mapped with ground surveys, geophysics, deep drilling, and repeat airborne lidar, The Cryosphere, 15, 3555-3575, 10.5194/tc-15-3555-2021, 2021.

Farquharson, L. M., Romanovsky, V. E., Cable, W. L., Walker, D. A., Kokelj, S. V., and Nicolsky, D.: Climate Change Drives Widespread and Rapid Thermokarst Development in Very Cold Permafrost in

带格式的：字体：10 磅
带格式的：标题 1，左，段落间距段前：24 磅，段后：12 磅
带格式的：字体：10 磅，非加粗，字体颜色：文字 1
带格式的：字体：10 磅，字体颜色：文字 1
带格式的：正文，左，段落间距段前：0.5 行，段后：0.5 行
带格式的：字体：10 磅
带格式的：字体：11 磅，字体颜色：文字 1
带格式的：字体：11 磅，非加粗，字体颜色：文字 1
带格式的：标题 1，左，段落间距段前：24 磅，段后：12 磅
带格式的：正文，左，段落间距段前：0.5 行，段后：0.5 行
带格式的：字体颜色：黑色
带格式的：字体颜色：黑色
带格式的：字体颜色：黑色
带格式的：字体颜色：灰色-80%，图案：清除（白色）
带格式的：字体颜色：黑色
带格式的：字体颜色：黑色
带格式的：字体：Helvetica，字体颜色：黑色
带格式的：字体：10 磅
带格式的：标题 1，左，段落间距段前：24 磅，段后：12 磅
带格式的：字体：10 磅

the Canadian High Arctic, Geophysical Research Letters, 46, 6681-6689, https://doi.org/10.1029/2019GL082187, 2019.

Grebenets, V. I., Tolmanov, V. A., and Streletskiy, D. A.: Active Layer Dynamics Near Norilsk, Taimyr Peninsula, Russia, Geography, Environment, Sustainability, 14, 55-66, 10.24057/2071-9388-2021-073, 2021.

Gruber, S.: Derivation and analysis of a high-resolution estimate of global permafrost zonation, The Cryosphere, 6, 10.5194/tc-6-221-2012, 2012.

Guglielmin, M.: Ground surface temperature (GST), active layer and permafrost monitoring in continental Antarctica, Permafrost and Periglacial Processes, 17, 133-143, https://doi.org/10.1002/ppp.553, 2006.

Guglielmin, M., Worland, M. R., and Cannone, N.: Spatial and temporal variability of ground surface temperature and active layer thickness at the margin of maritime Antarctica, Signy Island, Geomorphology, 155-156, 20-33, https://doi.org/10.1016/j.geomorph.2011.12.016, 2012.

Guo, W., Liu, H., Anenkhonov, O. A., Shangguan, H., Sandanov, D. V., Korolyuk, A. Y., Hu, G., and Wu, X.: Vegetation can strongly regulate permafrost degradation at its southern edge through changing surface freeze-thaw processes, Agricultural and Forest Meteorology, 252, 10-17, https://doi.org/10.1016/j.agrformet.2018.01.010, 2018.

He, R.-X., Jin, H.-J., Luo, D.-L., Li, X.-Y., Zhou, C.-F., Jia, N., Jin, X.-Y., Li, X.-Y., Che, T., Yang, X., Wang, L.-Z., Li, W.-H., Wei, C.-L., Chang, X.-L., and Yu, S.-P.: Permafrost changes in the Nanwenghe Wetlands Reserve on the southern slope of the Da Xing'anling–Yile'huli mountains, Northeast China, Advances in Climate Change Research, 12, 696-709, https://doi.org/10.1016/j.accre.2021.06.007, 2021.

Hrbáček, F., Vieira, G., Oliva, M., Balks, M., Guglielmin, M., de Pablo, M. Á., Molina, A., Ramos, M., Goyanes, G., Meiklejohn, I., Abramov, A., Demidov, N., Fedorov-Davydov, D., Lupachev, A., Rivkina, E., Láska, K., Kňažková, M., Nývlt, D., Raffi, R., Strelin, J., Sone, T., Fukui, K., Dolgikh, A., Zazovskaya, E., Mergelov, N., Osokin, N., and Miamin, V.: Active layer monitoring in Antarctica: an overview of results from 2006 to 2015, Polar Geography, 44, 217-231, 10.1080/1088937X.2017.1420105, 2021.

Jin, H., Wu, Q., and Romanovsky, V.: Degrading permafrost and its impacts, Advances in Climate Change Research, 12, 10.1016/j.accre.2021.01.007, 2021.

Jin, H., Li, S., Cheng, G., Shaoling, W., and Li, X.: Permafrost and climatic change in China, Global and Planetary Change, 26, 387-404, https://doi.org/10.1016/S0921-8181(00)00051-5, 2000.

Jin, H., Yu, Q., Lü, L., Guo, D., He, R., Yu, S.-p., Sun, G., and Li, Y.: Degradation of permafrost in the Xing'anling Mountains, northeastern China, Permafrost and Periglacial Processes, 18, 245-258, 2007.

Li, X.-Y., Jin, H.-J., Wang, H.-W., Marchenko, S. S., Shan, W., Luo, D.-L., He, R.-X., Spektor, V., Huang, Y.-D., Li, X.-Y., and Jia, N.: Influences of forest fires on the permafrost environment: A review, Advances in Climate Change Research, 12, 48-65, https://doi.org/10.1016/j.accre.2021.01.001, 2021.

Li, X., Jin, H., He, R., Huang, Y., Wang, H., Luo, D., Jin, X., Lü, L., Wang, L., Li, W. h., Wei, C., Chang, X., Yang, S., and Yu, S.: Effects of forest fires on the permafrost environment in the northern Da Xing'anling (Hinggan) mountains, Northeast China, Permafrost and Periglacial Processes, 30, 163-177, https://doi.org/10.1002/ppp.2001, 2019.

Luo, L., Ma, W., Zhuang, Y., Zhang, Y., Yi, S., Xu, J., Long, Y., Ma, D., and Zhang, Z.: The impacts of climate change and human activities on alpine vegetation and permafrost in the Qinghai-Tibet Engineering Corridor, Ecological Indicators, 93, 24-35, https://doi.org/10.1016/j.ecolind.2018.04.067, 2018.

Romanovsky, V. E., Smith, S. L., and Christiansen, H. H.: Permafrost thermal state in the polar Northern Hemisphere during the international polar year 2007–2009: a synthesis, Permafrost and Periglacial Processes, 21, 106-116, https://doi.org/10.1002/ppp.689, 2010.

Serban, R., Serban, M., He, R., Jin, H., Yan, L., Xinyu, L., Wang, X., and Li, G.: 46-Year (1973–2019) Permafrost Landscape Changes in the Hola Basin, Northeast China Using Machine Learning and Object-Oriented Classification, Remote Sensing, 13, 1910, 10.3390/rs13101910, 2021.

ShanShan Chen, S. Z., Li Sun: Characteristics of permafrost degradation in Northeast China and its ecological effects: A review, Sciences in Cold and Arid Regions, 12, 1-11, 10.3724/sp.j.1226.2020.00001., 2020.

Shiklomanov, N., Streletskiy, D., and Nelson, F.: Northern Hemisphere Component of the Global Circumpolar Active Layer Monitoring (CALM) Program, 2012.

Shur, Y. and Jorgenson, M.: Patterns of Permafrost Formation and Degradation in Relation to Climate and Ecosystems, Permafrost and Periglacial Processes, 18, 7-19, 10.1002/ppp.582, 2007.

Sim, T. G., Swindles, G. T., Morris, P. J., Baird, A. J., Cooper, C. L., Gallego-Sala, A. V., Charman, D. J., Roland, T. P., Borken, W., Mullan, D. J., Aquino-López, M. A., and Gałka, M.: Divergent responses of permafrost peatlands to recent climate change, Environmental Research Letters, 16, 034001, 10.1088/1748-9326/abe00b, 2021.

Smith, S. L., Romanovsky, V. E., Lewkowicz, A. G., Burn, C. R., Allard, M., Clow, G. D., Yoshikawa, K., and Throop, J.: Thermal state of permafrost in North America: a contribution to the international polar year, Permafrost and Periglacial Processes, 21, 117-135, https://doi.org/10.1002/ppp.690, 2010.

Wei, Z., Jin, H., Zhang, J., Yu, S., Han, X., Ji, Y., He, R., and Chang, X.: Prediction of permafrost changes in Northeastern China under a changing climate, Science China Earth Sciences, 54, 924-935, 10.1007/s11430-010-4109-6, 2011.

Yang, S. and Jin, H.: δ18O and δD records of inactive ice-wedge in Yitulihe, Northeastern China and their paleoclimatic implications, Science China Earth Sciences, 54, 119-126, 10.1007/s11430-010-4029-5, 2011.

Youhua, R., Cheng, G., Zhang, T., Wu, Q., Jin, H., and Jin, R.: Distribution of Permafrost in China: An Overview of Existing Permafrost Maps, Permafrost and Periglacial Processes, 23, 322-333, 10.1002/ppp.1756, 2012.

Zhang, G., Nan, Z., Wu, X., Ji, H., and Zhao, S.: The Role of Winter Warming in Permafrost Change Over the Qinghai-Tibet Plateau, Geophysical Research Letters, 46, 11261-11269, https://doi.org/10.1029/2019GL084292, 2019.

Zhang, T., Nelson, F., and Gruber, S.: Introduction to special section: Permafrost and Seasonally Frozen Ground Under a Changing Climate, Journal of Geophysical Research, 112, 10.1029/2007JF000821, 2007.

Zhang, Z.-Q., Wu, Q.-B., Hou, M.-T., Tai, B.-W., and An, Y.-K.: Permafrost change in Northeast China in the 1950s–2010s, Advances in Climate Change Research, 12, 18-28, https://doi.org/10.1016/j.accre.2021.01.006, 2021.

Zhang, Z., Wu, Q., Xun, X., Wang, B., and Wang, X.: Climate change and the distribution of frozen soil in 1980–2010 in northern northeast China, Quaternary International, 467, 230-241, https://doi.org/10.1016/j.quaint.2018.01.015, 2018.

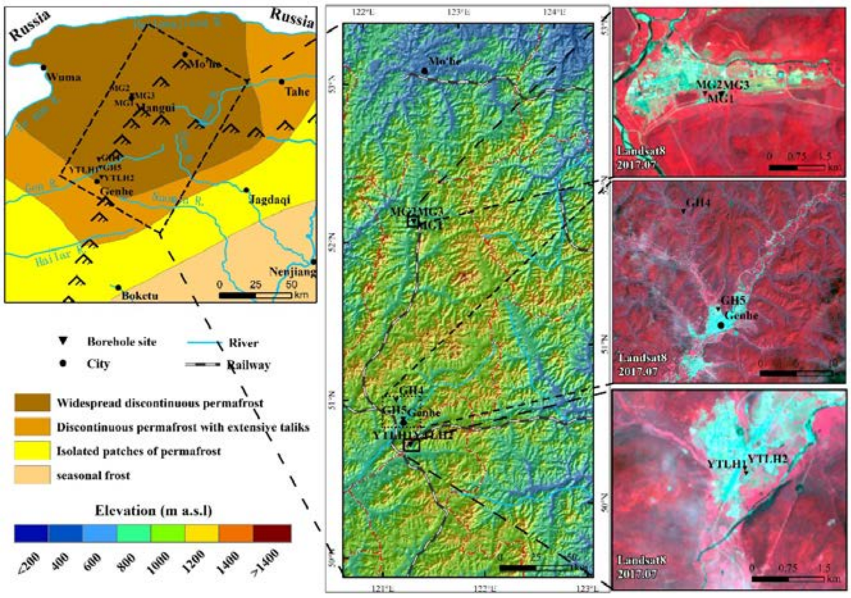

Ala-Aho, P., Autio, A., Bhattacharjee, J., Isokangas, E., Kujala, K., Marttila, H., Menberu, M., Meriö, L. J., Postila, H., Rauhala, A., Ronkanen, A. K., Rossi, P. M., Saari, M., Haghighi, A. T., and Kløve, B.: What conditions favor the influence of seasonally frozen ground on hydrological partitioning? A systematic review, Environmental Research Letters, 16, 043008, 10.1088/1748-9326/abe82c, 2021.

Baltzer, J. L., Veness, T., Chasmer, L. E., Sniderhan, A. E., and Quinton, W. L.: Forests on thawing permafrost: fragmentation, edge effects, and net forest loss, Global change biology, 20, 824-834, 10.1111/gcb.12349, 2014.

Beer, C., Zimov, N., Olofsson, J., Porada, P., and Zimov, S.: Protection of Permafrost Soils from Thawing by Increasing Herbivore Density, Scientific reports, 10, 4170, 10.1038/s41598-020-60938-y, 2020.

Biskaborn, B. K., Smith, S. L., Noetzli, J., Matthes, H., Vieira, G., Streletskiy, D. A., Schoeneich, P., Romanovsky, V. E., Lewkowicz, A. G., Abramov, A., Allard, M., Boike, J., Cable, W. L., Christiansen, H. H., Delaloye, R., Diekmann, B., Drozdov, D., Etzelmüller, B., Grosse, G., Guglielmin, M., Ingeman-Nielsen, T., Isaksen, K., Ishikawa, M., Johansson, M., Johannsson, H., Joo, A., Kaverin, D., Kholodov, A., Konstantinov, P., Kröger, T., Lambiel, C., Lanckman, J.-P., Luo, D., Malkova, G., Meiklejohn, I., Moskalenko, N., Oliva, M., Phillips, M., Ramos, M., Sannel, A. B. K., Sergeev, D., Seybold, C., Skryabin, P., Vasiliev, A., Wu, Q., Yoshikawa, K., Zheleznyak, M., and Lantuit, H.: Permafrost is warming at a global scale, Nature Communications, 10, 264, 10.1038/s41467-018-08240-4, 2019.

Briggs, M. A., Walvoord, M. A., McKenzie, J. M., Voss, C. I., Day-Lewis, F. D., and Lane, J. W.: New permafrost is forming around shrinking Arctic lakes, but will it last?, Geophysical Research Letters, 41, 1585-1592, https://doi.org/10.1002/2014GL059251, 2014.

Brown, D. R. N., Jorgenson, M. T., Douglas, T. A., Romanovsky, V. E., Kielland, K., Hiemstra, C., Euskirchen, E. S., and Ruess, R. W.: Interactive effects of wildfire and climate on permafrost degradation in Alaskan lowland forests, Journal of Geophysical Research: Biogeosciences, 120, 1619-1637, https://doi.org/10.1002/2015JG003033, 2015.

Brown, J., Hinkel, K. M., and Nelson, F. E.: The circumpolar active layer monitoring (calm) program:

Research designs and initial results, Polar Geography, 24, 166-258, 10.1080/10889370009377698, 2000.

Cao, B., Zhang, T., Wu, Q., Sheng, Y., Zhao, L., and Zou, D.: Permafrost zonation index map and statistics over the Qinghai-Tibet Plateau based on field evidence, Permafrost and Periglacial Processes, 30, 178-194, 10.1002/ppp.2006, 2019.

Cao, B., Zhang, T., Peng, X., Mu, C., Wang, Q., Zheng, L., Wang, K., and Zhong, X.: Thermal Characteristics and Recent Changes of Permafrost in the Upper Reaches of the Heihe River Basin, Western China, Journal of Geophysical Research: Atmospheres, 123, 7935-7949, https://doi.org/10.1029/2018JD028442, 2018.

Chen, S.-S., Zang, S., and Sun, L.: Characteristics of permafrost degradation in Northeast China and its ecological effects: A review, Sciences in Cold and Arid Regions, 12, 1-11, 10.3724/sp.j.1226.2020.00001., 2020.

Douglas, T. A., Hiemstra, C. A., Anderson, J. E., Barbato, R. A., Bjella, K. L., Deeb, E. J., Gelvin, A. B., Nelsen, P. E., Newman, S. D., Saari, S. P., and Wagner, A. M.: Recent degradation of interior Alaska permafrost mapped with ground surveys, geophysics, deep drilling, and repeat airborne lidar, The Cryosphere, 15, 3555-3575, 10.5194/tc-15-3555-2021, 2021.

Everdingen, R. O. v.: Multi-language glossary of permafrost and related ground-ice terms, National Snow and Ice Data Centre, Boulder, CO1998 (revised 2005).

Farquharson, L. M., Romanovsky, V. E., Cable, W. L., Walker, D. A., Kokelj, S. V., and Nicolsky, D.: Climate Change Drives Widespread and Rapid Thermokarst Development in Very Cold Permafrost in the Canadian High Arctic, Geophysical Research Letters, 46, 6681-6689, https://doi.org/10.1029/2019GL082187, 2019.

Grebenets, V. I., Tolmanov, V. A., and Streletskiy, D. A.: Active Layer Dynamics Near Norilsk, Taimyr Peninsula, Russia, Geography, Environment, Sustainability, 14, 55-66, 10.24057/2071-9388-2021-073, 2021.

Gruber, S.: Derivation and analysis of a high-resolution estimate of global permafrost zonation, The Cryosphere, 6, 10.5194/tc-6-221-2012, 2012.

Guglielmin, M.: Ground surface temperature (GST), active layer and permafrost monitoring in continental Antarctica, Permafrost and Periglacial Processes, 17, 133-143, https://doi.org/10.1002/ppp.553, 2006.

Guglielmin, M., Worland, M. R., and Cannone, N.: Spatial and temporal variability of ground surface temperature and active layer thickness at the margin of maritime Antarctica, Signy Island, Geomorphology, 155-156, 20-33, https://doi.org/10.1016/j.geomorph.2011.12.016, 2012.

Guo, W., Liu, H., Anenkhonov, O. A., Shangguan, H., Sandanov, D. V., Korolyuk, A. Y., Hu, G., and Wu, X.: Vegetation can strongly regulate permafrost degradation at its southern edge through changing surface freeze-thaw processes, Agricultural and Forest Meteorology, 252, 10-17, https://doi.org/10.1016/j.agrformet.2018.01.010, 2018.

He, R.-X., Jin, H.-J., Luo, D.-L., Li, X.-Y., Zhou, C.-F., Jia, N., Jin, X.-Y., Li, X.-Y., Che, T., Yang, X., Wang, L.-Z., Li, W.-H., Wei, C.-L., Chang, X.-L., and Yu, S.-P.: Permafrost changes in the Nanwenghe Wetlands Reserve on the southern slope of the Da Xing'anling–Yile'huli mountains, Northeast China, Advances in Climate Change Research, 12, 696-709, https://doi.org/10.1016/j.accre.2021.06.007, 2021.

Hrbáček, F., Vieira, G., Oliva, M., Balks, M., Guglielmin, M., de Pablo, M. Á., Molina, A., Ramos, M., Goyanes, G., Meiklejohn, I., Abramov, A., Demidov, N., Fedorov-Davydov, D., Lupachev, A., Rivkina, E., Láska, K., Kňažková, M., Nývlt, D., Raffi, R., Strelin, J., Sone, T., Fukui, K., Dolgikh, A., Zazovskaya, E., Mergelov, N., Osokin, N., and Miamin, V.: Active layer monitoring in Antarctica: an overview of results from 2006 to 2015, Polar Geography, 44, 217-231, 10.1080/1088937X.2017.1420105, 2021.

Jin, H., Wu, Q., and Romanovsky, V.: Degrading permafrost and its impacts, Advances in Climate Change Research, 12, 10.1016/j.accre.2021.01.007, 2021.

Jin, H., Li, S., Cheng, G., Shaoling, W., and Li, X.: Permafrost and climatic change in China, Global and Planetary Change, 26, 387-404, https://doi.org/10.1016/S0921-8181(00)00051-5, 2000.

Jin, H., Yu, Q., Lü, L., Guo, D., He, R., Yu, S.-p., Sun, G., and Li, Y.: Degradation of permafrost in the Xing'anling Mountains, northeastern China, Permafrost and Periglacial Processes, 18, 245-258, 2007.

Li, X.-Y., Jin, H.-J., Wang, H.-W., Marchenko, S. S., Shan, W., Luo, D.-L., He, R.-X., Spektor, V., Huang, Y.-D., Li, X.-Y., and Jia, N.: Influences of forest fires on the permafrost environment: A review, Advances in Climate Change Research, 12, 48-65, https://doi.org/10.1016/j.accre.2021.01.001, 2021.

Li, X., Jin, H., He, R., Huang, Y., Wang, H., Luo, D., Jin, X., Lü, L., Wang, L., Li, W. h., Wei, C., Chang, X., Yang, S., and Yu, S.: Effects of forest fires on the permafrost environment in the northern Da Xing'anling (Hinggan) mountains, Northeast China, Permafrost and Periglacial Processes, 30, 163-177, https://doi.org/10.1002/ppp.2001, 2019.

Luo, L., Ma, W., Zhuang, Y., Zhang, Y., Yi, S., Xu, J., Long, Y., Ma, D., and Zhang, Z.: The impacts of climate change and human activities on alpine vegetation and permafrost in the Qinghai-Tibet Engineering Corridor, Ecological Indicators, 93, 24-35, https://doi.org/10.1016/j.ecolind.2018.04.067, 2018.

Mu, C., Abbott, B. W., Norris, A. J., Mu, M., Fan, C., Chen, X., Jia, L., Yang, R., Zhang, T., Wang, K., Peng, X., Wu, Q., Guggenberger, G., and Wu, X.: The status and stability of permafrost carbon on the Tibetan Plateau, Earth-Science Reviews, 211, 103433, 10.1016/j.earscirev.2020.103433, 2020.

Ran, Y., Li, X., and Cheng, G.: Climate warming over the past half century has led to thermal degradation of permafrost on the Qinghai–Tibet Plateau, The Cryosphere, 12, 595-608, 10.5194/tc-12-595-2018, 2018.

Ran, Y., Li, X., Cheng, G., Che, J., Aalto, J., Karjalainen, O., Hjort, J., Luoto, M., Jin, H., Obu, J., Hori, M., Yu, Q., and Chang, X.: New high-resolution estimates of the permafrost thermal state and hydrothermal conditions over the Northern Hemisphere, Earth Syst. Sci. Data, 14, 865-884, 10.5194/essd-14-865-2022, 2022.

Romanovsky, V. E., Smith, S. L., and Christiansen, H. H.: Permafrost thermal state in the polar Northern Hemisphere during the international polar year 2007–2009: a synthesis, Permafrost and Periglacial Processes, 21, 106-116, https://doi.org/10.1002/ppp.689, 2010.

Schuur, E. A. G. and Mack, M. C.: Ecological Response to Permafrost Thaw and Consequences for Local and Global Ecosystem Services, Annual Review of Ecology, Evolution, and Systematics, 49, 279-301, 10.1146/annurev-ecolsys-121415-032349, 2018.

Schuur, E. A. G., McGuire, A. D., Schädel, C., Grosse, G., Harden, J. W., Hayes, D. J., Hugelius, G., Koven, C. D., Kuhry, P., Lawrence, D. M., Natali, S. M., Olefeldt, D., Romanovsky, V. E., Schaefer, K., Turetsky, M. R., Treat, C. C., and Vonk, J. E.: Climate change and the permafrost carbon feedback, Nature, 520, 171-179, 10.1038/nature14338, 2015.

Serban, R., Serban, M., He, R., Jin, H., Yan, L., Xinyu, L., Wang, X., and Li, G.: 46-Year (1973–2019) Permafrost Landscape Changes in the Hola Basin, Northeast China Using Machine Learning and Object-Oriented Classification, Remote Sensing, 13, 1910, 10.3390/rs13101910, 2021.

Shiklomanov, N., Streletskiy, D., and Nelson, F.: Northern Hemisphere Component of the Global

Circumpolar Active Layer Monitoring (CALM) Program, 2012.

Shur, Y. and Jorgenson, M.: Patterns of Permafrost Formation and Degradation in Relation to Climate and Ecosystems, Permafrost and Periglacial Processes, 18, 7-19, 10.1002/ppp.582, 2007.

Sim, T. G., Swindles, G. T., Morris, P. J., Baird, A. J., Cooper, C. L., Gallego-Sala, A. V., Charman, D. J., Roland, T. P., Borken, W., Mullan, D. J., Aquino-López, M. A., and Gałka, M.: Divergent responses of permafrost peatlands to recent climate change, Environmental Research Letters, 16, 034001, 10.1088/1748-9326/abe00b, 2021.

Smith, S. L., Romanovsky, V. E., Lewkowicz, A. G., Burn, C. R., Allard, M., Clow, G. D., Yoshikawa, K., and Throop, J.: Thermal state of permafrost in North America: a contribution to the international polar year, Permafrost and Periglacial Processes, 21, 117-135, https://doi.org/10.1002/ppp.690, 2010.

Wei, Z., Jin, H., Zhang, J., Yu, S., Han, X., Ji, Y., He, R., and Chang, X.: Prediction of permafrost changes in Northeastern China under a changing climate, Science China Earth Sciences, 54, 924-935, 10.1007/s11430-010-4109-6, 2011.

Yang, S. and Jin, H.: δ18O and δD records of inactive ice wedge in Yitulihe, Northeastern China and their paleoclimatic implications, Science China Earth Sciences, 54, 119-126, 10.1007/s11430-010-4029-5, 2011.

Zhang, G., Nan, Z., Wu, X., Ji, H., and Zhao, S.: The Role of Winter Warming in Permafrost Change Over the Qinghai-Tibet Plateau, Geophysical Research Letters, 46, 11261-11269, https://doi.org/10.1029/2019GL084292, 2019.

Zhang, T., Nelson, F., and Gruber, S.: Introduction to special section: Permafrost and Seasonally Frozen Ground Under a Changing Climate, Journal of Geophysical Research, 112, 10.1029/2007JF000821, 2007.

Zhang, Y., Cheng, G., Jin, H., Yang, D., Flerchinger, G., Chang, X., Wang, X., and Liang, J.: Influences of Topographic Shadows on the Thermal and Hydrological Processes in a Cold Region Mountainous Watershed in Northwest China, Journal of Advances in Modeling Earth Systems, 10, 10.1029/2017MS001264, 2018a.

Zhang, Y., Cheng, G., Jin, H., Yang, D., Flerchinger, G., Chang, X., Bense, V., Han, X., and Liang, J.: Influences of frozen ground and climate change on the hydrological processes in an alpine watershed: A case study in the upstream area of the Hei'he River, Northwest China, Permafrost and Periglacial Processes, 28, 420-432, 2017.

Zhang, Z.-Q., Wu, Q.-B., Hou, M.-T., Tai, B.-W., and An, Y.-K.: Permafrost change in Northeast China in the 1950s–2010s, Advances in Climate Change Research, 12, 18-28, https://doi.org/10.1016/j.accre.2021.01.006, 2021.

Zhang, Z., Wu, Q., Xun, X., Wang, B., and Wang, X.: Climate change and the distribution of frozen soil in 1980–2010 in northern northeast China, Quaternary International, 467, 230-241, https://doi.org/10.1016/j.quaint.2018.01.015, 2018b.

Zou, D., Zhao, L., Sheng, Y., Chen, J., Hu, G., Wu, T., Wu, J., Xie, C., Wu, X., Pang, Q., Wang, W., Du, E., Li, W., Liu, G., Li, J., Qin, Y., Qiao, Y., Wang, Z., Shi, J., and Cheng, G.: A new map of permafrost distribution on the Tibetan Plateau, The Cryosphere, 11, 2527-2542, 10.5194/tc-11-2527-2017, 2017.

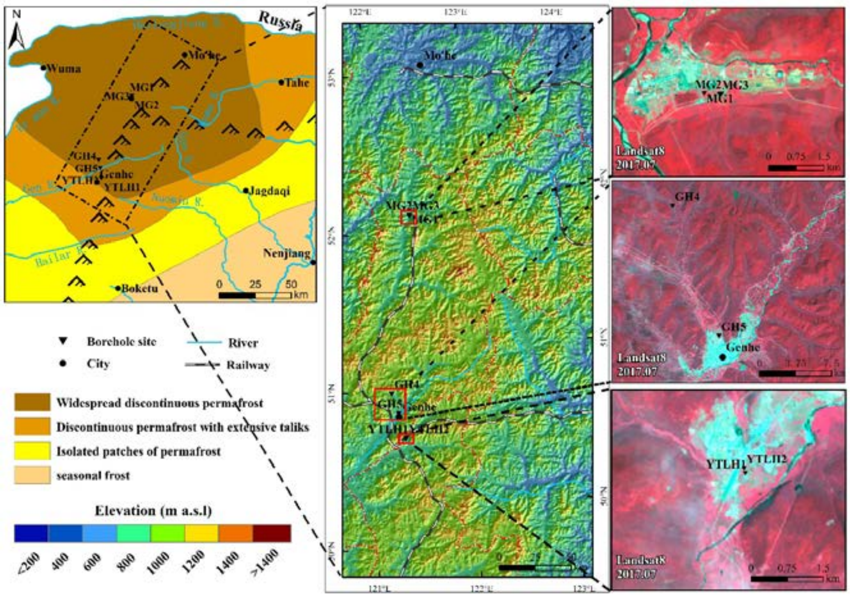

Figure 1. Location of the study area and the distribution of ~~borehole sites~~Mangui1 (MG1), Mangui2 (MG2), Mangui3 (MG3), Gen'he4 (GH4), Gen'he5 (GH5), Yituli'he1 (YTLH1) and Yituli'he2 (YTLH2) in the zones of frozen ground in the northern Da ~~Xing'anling~~Xing''anling Mountains, Northeast China (The permafrost distribution is from Jin et al. (2007).)

带格式的：字体：加粗

带格式的：两端对齐

带格式的：字体：加粗

带格式的：字体：加粗

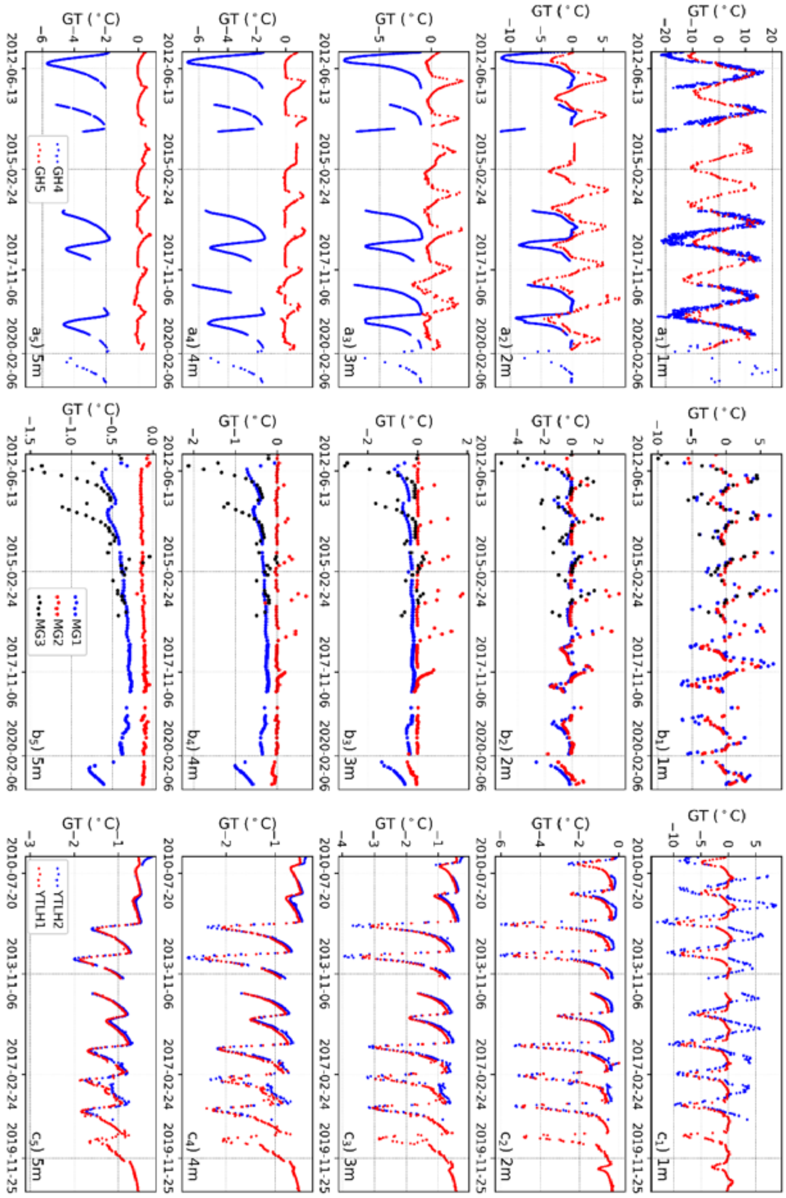

Figure 2. Variability of measured ground temperatures at depths of 1-5 m for Boreholes GH4 and GH5 (a)), MG1, MG2 and MG3 (b)), and YTLH1 and YTLH2 (c)).

带格式的：字体：9 磅，加粗

带格式的：两端对齐

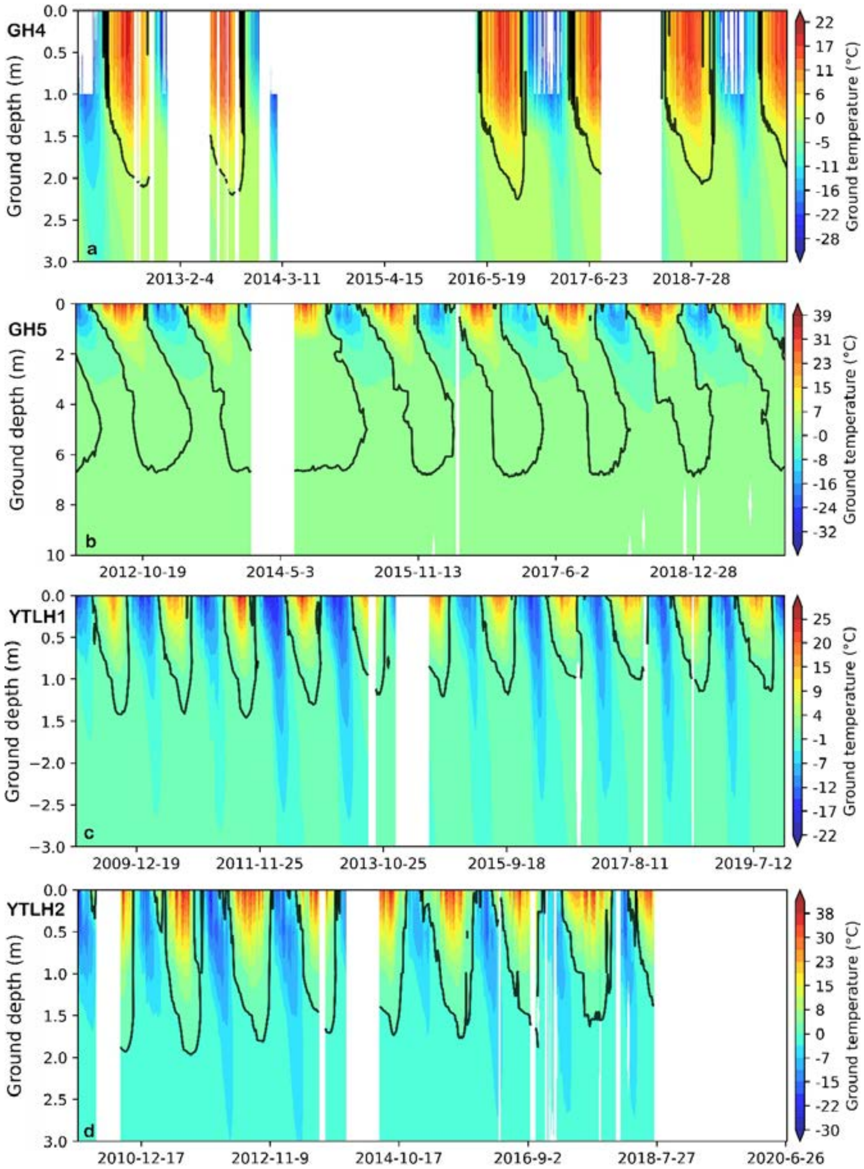

Figure 3 Variability of 0 °C isotherms (black curves) of ground temperature for Boreholes GH4 (a), GH5 (b), YTLH1 (c), and YTLH2 (d). The empty space indicates the period of missing data.

带格式的：字体：9 磅，加粗
带格式的：两端对齐

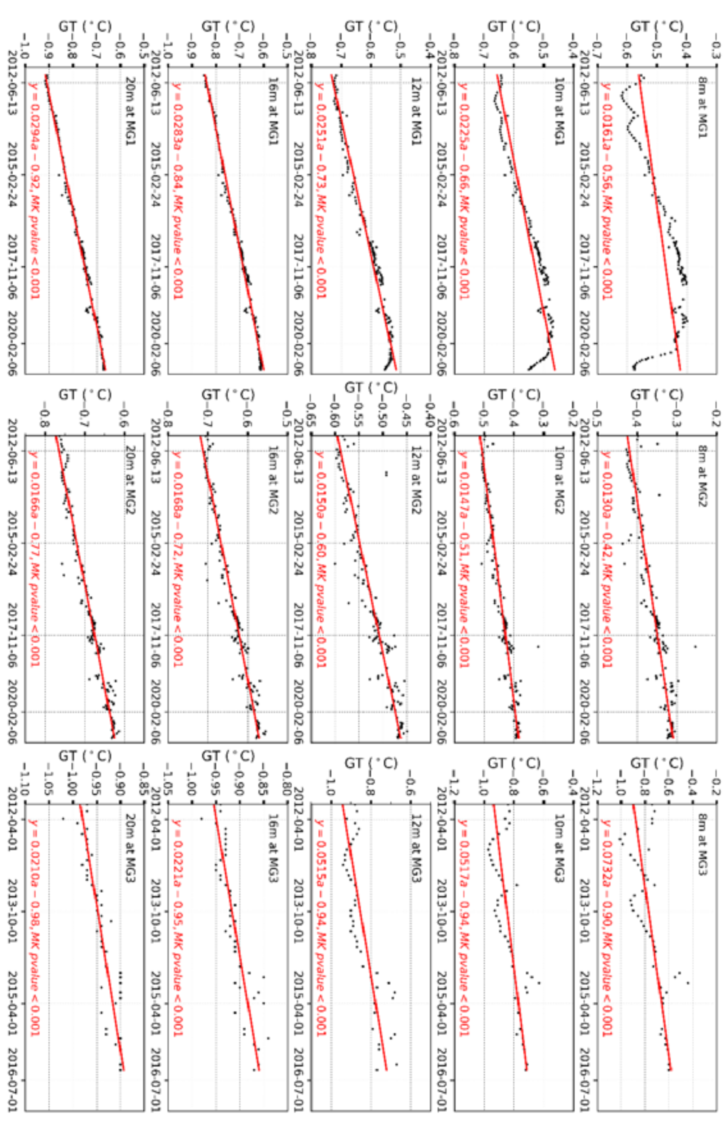
GT (°C)
8m at MG1
y = 0.0161a − 0.56, MK pvalue < 0.001
10m at MG1
y = 0.0225a − 0.66, MK pvalue < 0.001
12m at MG1
y = 0.0251a − 0.73, MK pvalue < 0.001
16m at MG1
y = 0.0283a − 0.84, MK pvalue < 0.001
20m at MG1
y = 0.0294a − 0.92, MK pvalue < 0.001
8m at MG2
y = 0.0130a − 0.42, MK pvalue < 0.001
10m at MG2
y = 0.0147a − 0.51, MK pvalue < 0.001
12m at MG2
y = 0.0150a − 0.60, MK pvalue < 0.001
16m at MG2
y = 0.0168a − 0.72, MK pvalue < 0.001
20m at MG2
y = 0.0166a − 0.77, MK pvalue < 0.001
8m at MG3
y = 0.0732a − 0.90, MK pvalue < 0.001
10m at MG3
y = 0.0517a − 0.94, MK pvalue < 0.001
12m at MG3
y = 0.0515a − 0.94, MK pvalue < 0.001
16m at MG3
y = 0.0221a − 0.95, MK pvalue < 0.001
20m at MG3
y = 0.0210a − 0.98, MK pvalue < 0.001

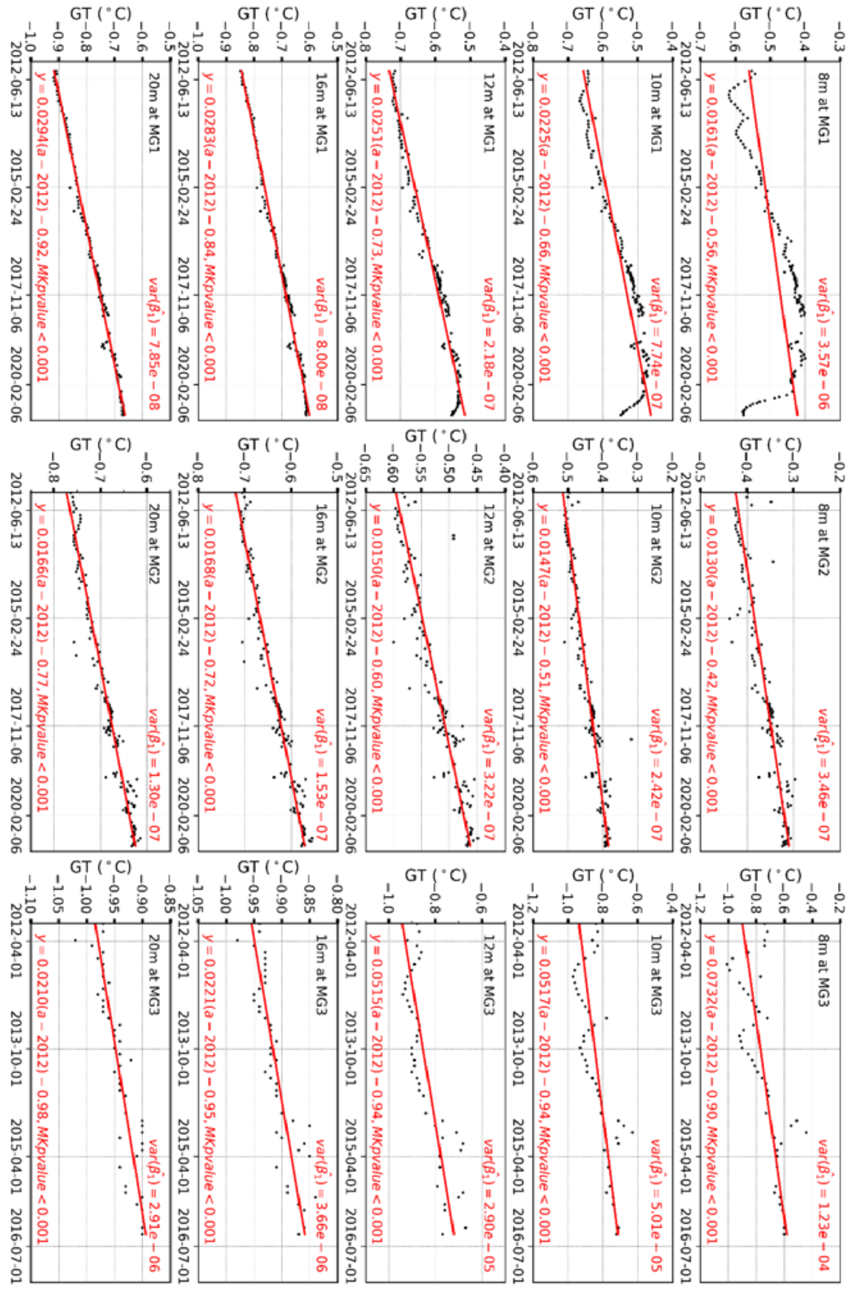

Figure 4. Variability of permafrost temperatures at depths of 8, 10, 12, 16 and 20 m in Boreholes MG1, MG2 and MG3 in Mangui, northern Da Xing'anling Mountains, Northeast China during 2012-2020. GT stands for ground temperature.

带格式的: 字体: 9 磅, 加粗

带格式的: 两端对齐

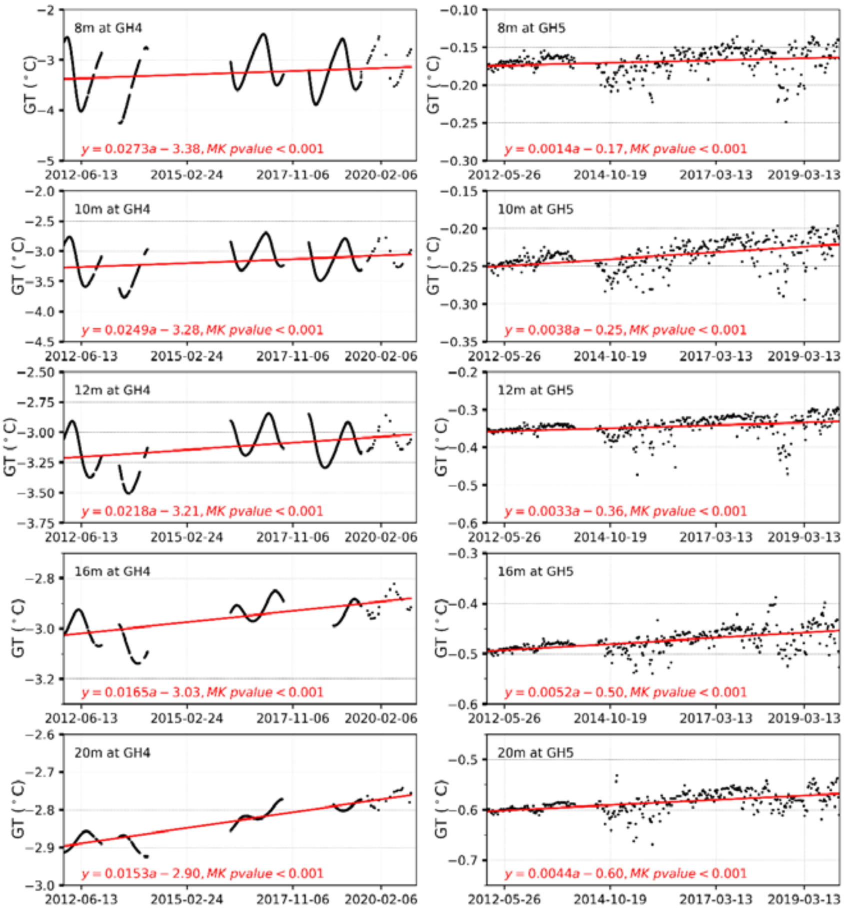
8m at GH4
y = 0.0273a − 3.38, MK pvalue < 0.001
8m at GH5
y = 0.0014a − 0.17, MK pvalue < 0.001
10m at GH4
y = 0.0249a − 3.28, MK pvalue < 0.001
10m at GH5
y = 0.0038a − 0.25, MK pvalue < 0.001
12m at GH4
y = 0.0218a − 3.21, MK pvalue < 0.001
12m at GH5
y = 0.0033a − 0.36, MK pvalue < 0.001
16m at GH4
y = 0.0165a − 3.03, MK pvalue < 0.001
16m at GH5
y = 0.0052a − 0.50, MK pvalue < 0.001
20m at GH4
y = 0.0153a − 2.90, MK pvalue < 0.001
20m at GH5
y = 0.0044a − 0.60, MK pvalue < 0.001
GT (°C)
2012-06-13
2015-02-24
2017-11-06
2020-02-06
2012-05-26
2014-10-19
2017-03-13
2019-03-13

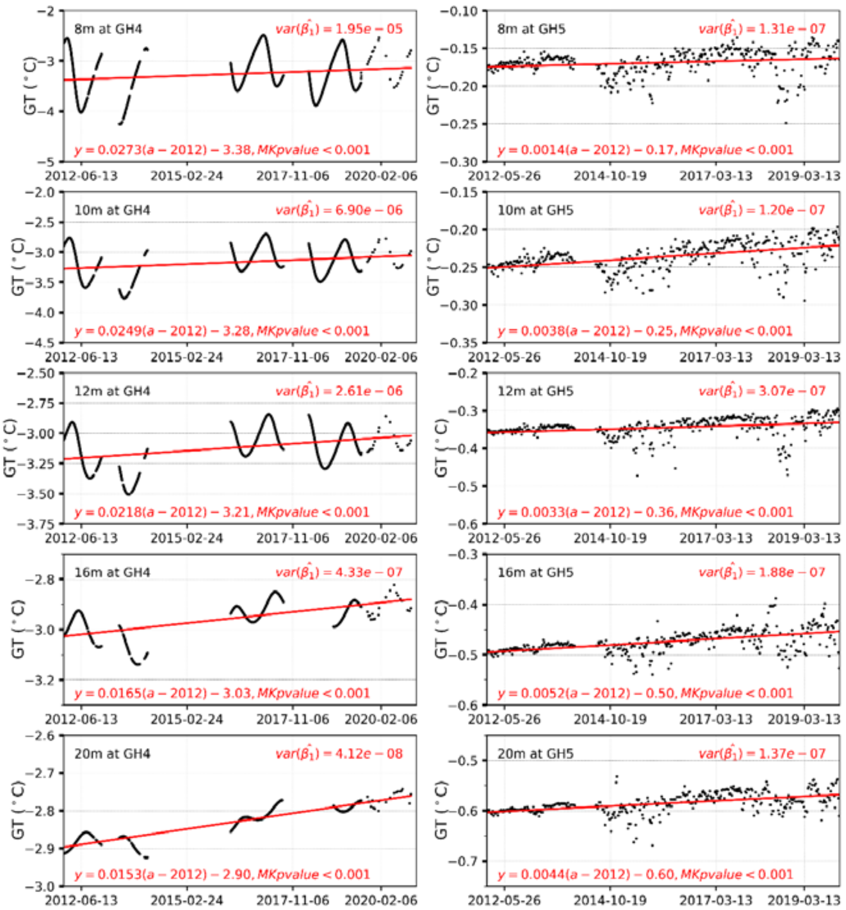

Figure 5. Variations in permafrost temperatures at depths of 8, 10, 12, 16 and 20 m in Boreholes GH4 and GH5 in Gen'he, northern Da Xing'anling Mountains, Northeast China during 2012-2020. GT stands for ground temperature.

带格式的：字体：9 磅，加粗

带格式的：两端对齐

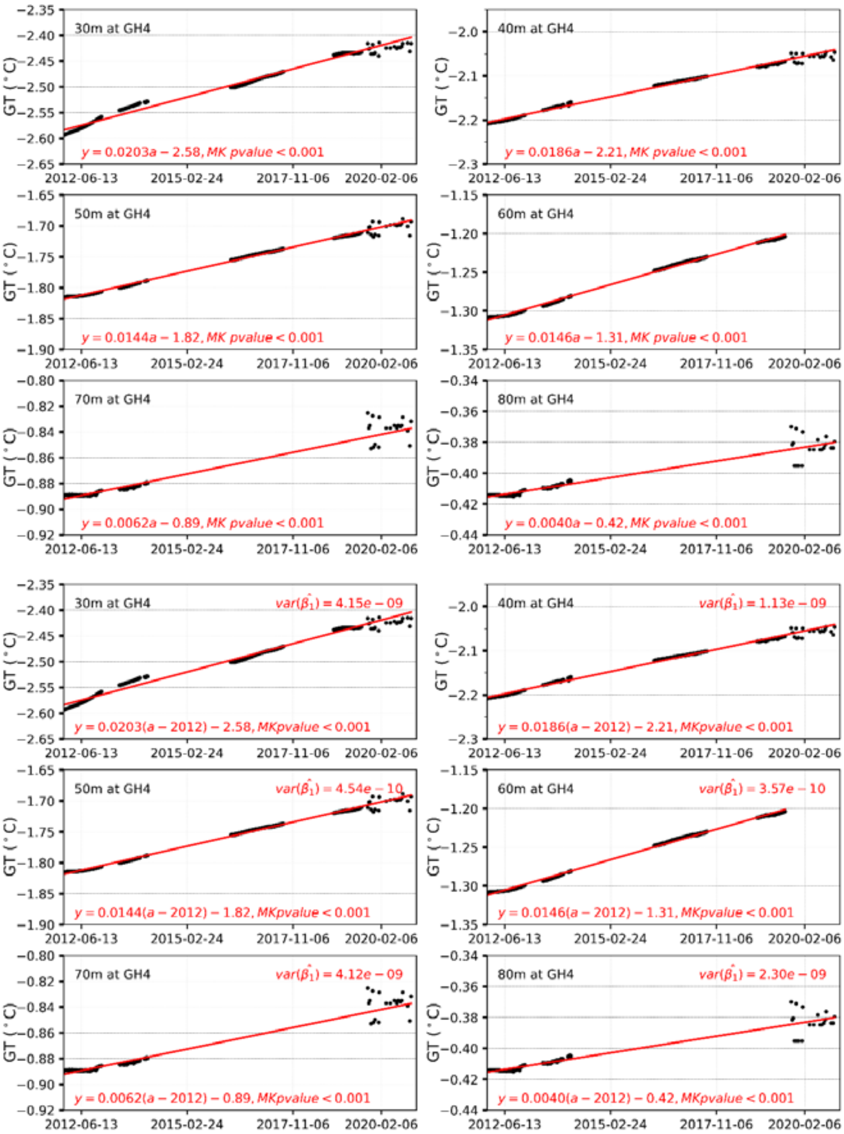

Figure 6. Variability of deep permafrost temperatures at depths of 30 – 80 m for Borehole GH4 in Gen'he, northern Da Xing'anling Mountains, Northeast China during 2012-2020. GT stands for ground temperature.

带格式的：字体：9 磅，加粗

带格式的：两端对齐

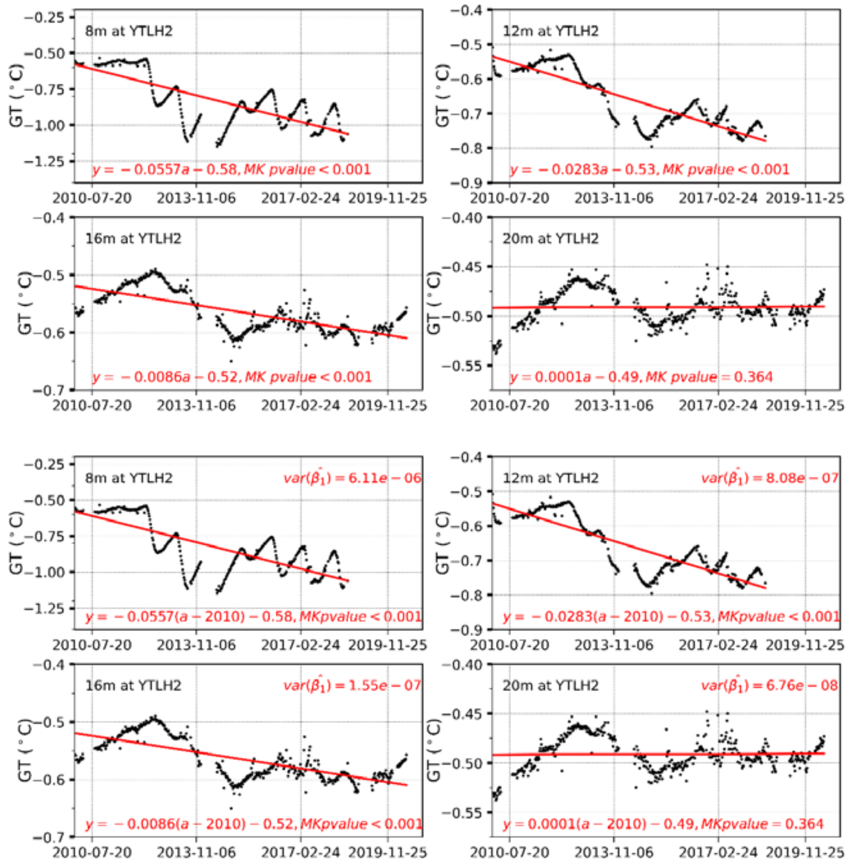

Figure 7. Variability of permafrost temperatures at depths of 8, 12, 16 and 20 m at Borehole YTLH2 in Yituli'he in northern Da Xing'anling Mountains, Northeast China during 2012-2020. GT stands for ground temperature.

带格式的：字体：9 磅，加粗

带格式的：两端对齐

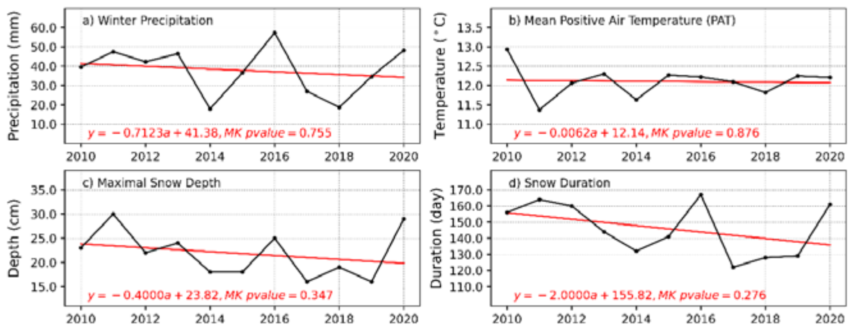

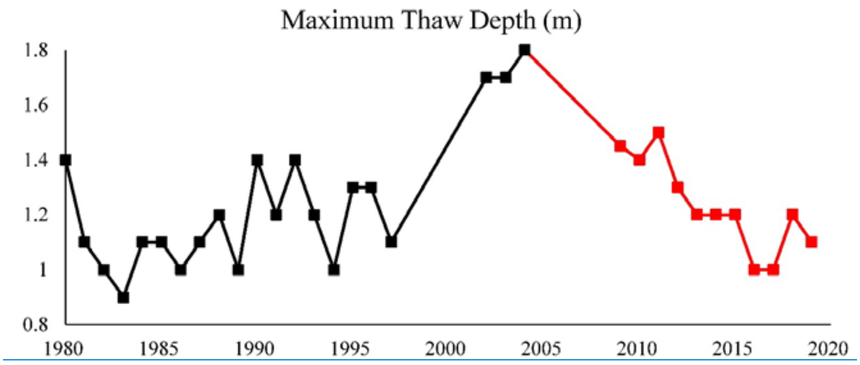

Figure 8. ~~Climatic characteristics of Gen'he on the northwestern flank of the northern Da Xing'anling Mountains in Northeast China in the past ten years~~

带格式的：字体：9 磅，加粗

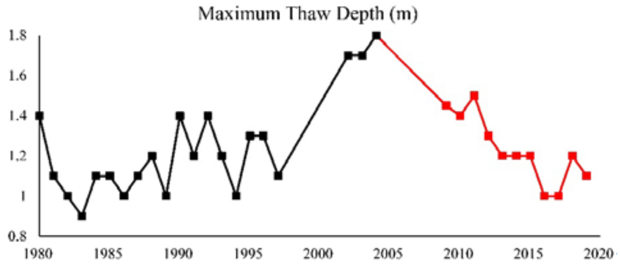

~~Figure 9.~~ **The maximum thaw depth (1980-2019) in Yituli'he on the northwestern flank of the northern Da Xing'anling Mountains in Northeast China** ~~between 1980-2020~~ **(Black squares appeared in the paper from Jin et al. (2007), red ones are obtained in this observation. The two boreholes are 10 m from each other, with similar surface, hydrology and soil conditions.)**

带格式的：字体：9 磅，加粗

带格式的：两端对齐

带格式的：字体：9 磅，加粗

带格式的：字体：9 磅，加粗

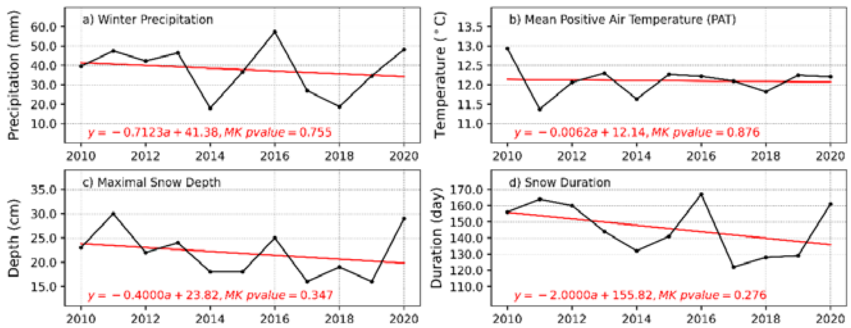

Figure 9. Climatic characteristics of Gen'he on the northwestern flank of the northern Da Xing'anling Mountains in Northeast China in the past ten years

带格式的：字体：9 磅，加粗

带格式的：两端对齐

Table 1. Characteristics and monitoring information of ground temperature boreholes in the northwestern part of Da Xing'anling Mountains, Northeastern China

Borehole No.	Lat. (°N)	Long. (°E)	Elev. (m a. s. l.)	Vegetation	Monitoring depths (m)	Time period	Monitoring frequency
MG1	52.037	122.069	633	*Betula fruticosa* shrubs		2012-2020	
MG2	52.036	122.075	642	*Carex tato* meadow	0.0, 1.0, 1.5, 2.0, 2.5, 3.0, 3.5, 4.0, 4.5, 5.0, 6.0, 7.0, 8.0, 9.0, 10.0, 11, 12, 13, 14, 15, 16, 17, 18, 19, 20	2012-2020	Monthly
MG3	52.036	122.076	639	Open courtyard		2012-2015	
GH4	50.932	121.502	811	*Betula fruticosa* *Larix gmelini* forest	0.0, 1.0, 1.5, 2.0, 2.5, 3.0, 3.5, 4.0, 4.5, 5.0, 6.0, 7.0, 8.0, 9.0, 10.0, 11, 12, 13, 14, 15, 16, 17, 18, 19, 20, 25, 30, 35, 40, 45, 50, 60, 70, 80	2012-2014, 2016-2017, 2019-2020	Hourly
GH5	50.799	121.530	728	*Carex tato* meadow	0.0, 1.0, 1.5, 2.0, 2.5, 3.0, 3.5, 4.0, 4.5, 5.0, 6.0, 7.0, 8.0, 9.0, 10.0, 11, 12, 13, 14, 15, 16, 17, 18, 19, 20	2012-2019	
~~YT1~~YT LH1	50.629	121.549	721	*Carex tato* swamp	0.0, 0.1, 0.2, 0.5, 0.8, 1.0, 1.6, 2.0, 3.0, 4.0, 5.0, 6.0, 7.0, 8.15	2009-2019	Weekly
~~YT2~~YT LH2	50.630	121.549	725	*Carex tato* swamp	0.0, 1.0, 1.5, 2.0, 2.5, 3.0, 3.5, 4.0, 4.5, 5.0, 6.0, 7.0, 8.0, 9.0, 10.0, 11, 12, 13, 14, 15, 16, 17, 18, 19, 20	2010-2017	

Table 2 ALT and average MAGTs of boreholes at larger depths in the northwestern Da Xing'anling Mountains, Northeast China

Borehole	ALT (m)	Average MAGT (°C)				
		8m	10m	13m	16m	20m
MG1	1.9-2.6	-0.48(ZAA)	-0.55	-0.63	-0.71	-0.77
MG2	4.3-4.8	-0.34(ZAA)	-0.44	-0.55	-0.63	-0.69
MG3	2.8-4.0	-0.75	-0.83	-0.87(ZAA)	-0.91	-0.94
GH4	2.0-2.2	-3.26	-3.17	-3.06	-2.96(ZAA)	-2.84
GH5	7.0	-0.17(ZAA)	-0.24	-0.39	-0.47	-0.59
YTLH2	1.5-2.0	-0.82	-0.74	-0.61(ZAA)	-0.56	-0.49